

Precision studies at FCC-hh

With diboson (Vh) production

FCC Phenomenology Workshop

6 July 2023

CERN, Switzerland

Alejo N. Rossia

Department of Physics and Astronomy

University of Manchester

With F. Bishara, S. De Curtis, L. Delle Rose, P. Englert, C. Grojean, M. Montull, G. Panico.

arXiv 2004.06122 (JHEP 07 (2020) 075)

arXiv 2011.13941 (JHEP 04 (2021) 154)

arXiv 2208.11134 (JHEP 06 (2023) 077)

MANCHESTER
1824

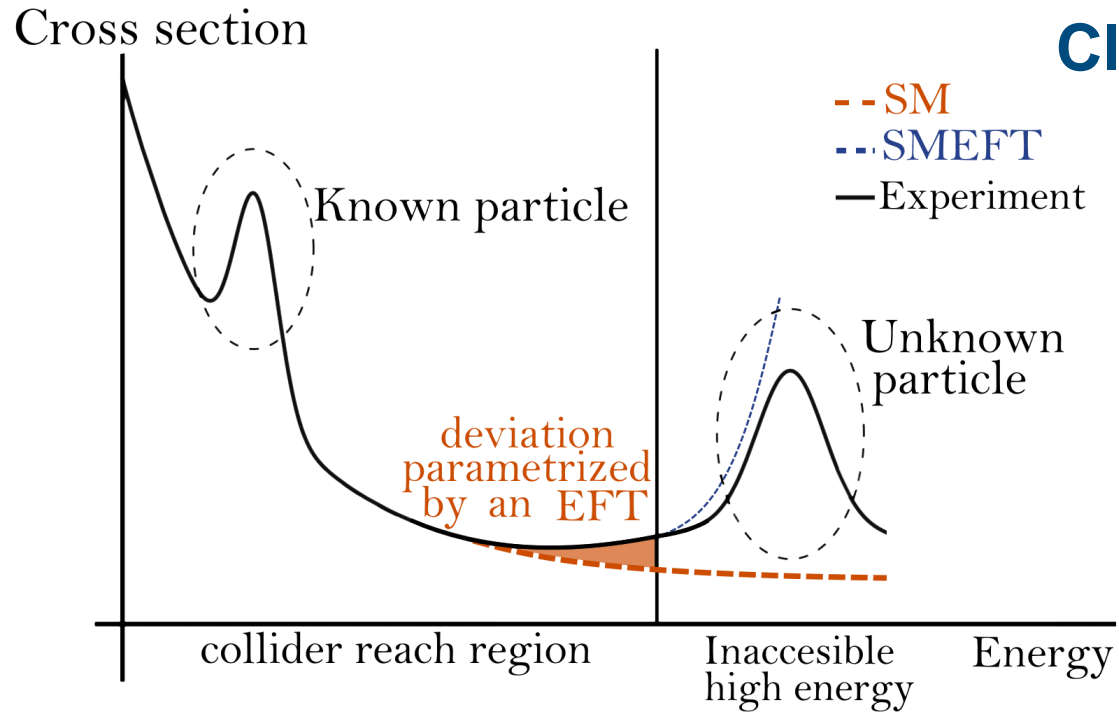
The University of Manchester

A trick of the tail

Precision with hadron colliders? Yes!

A trick of the tail

Precision with hadron colliders? Yes!



Clean channels + NP effects that grow with E

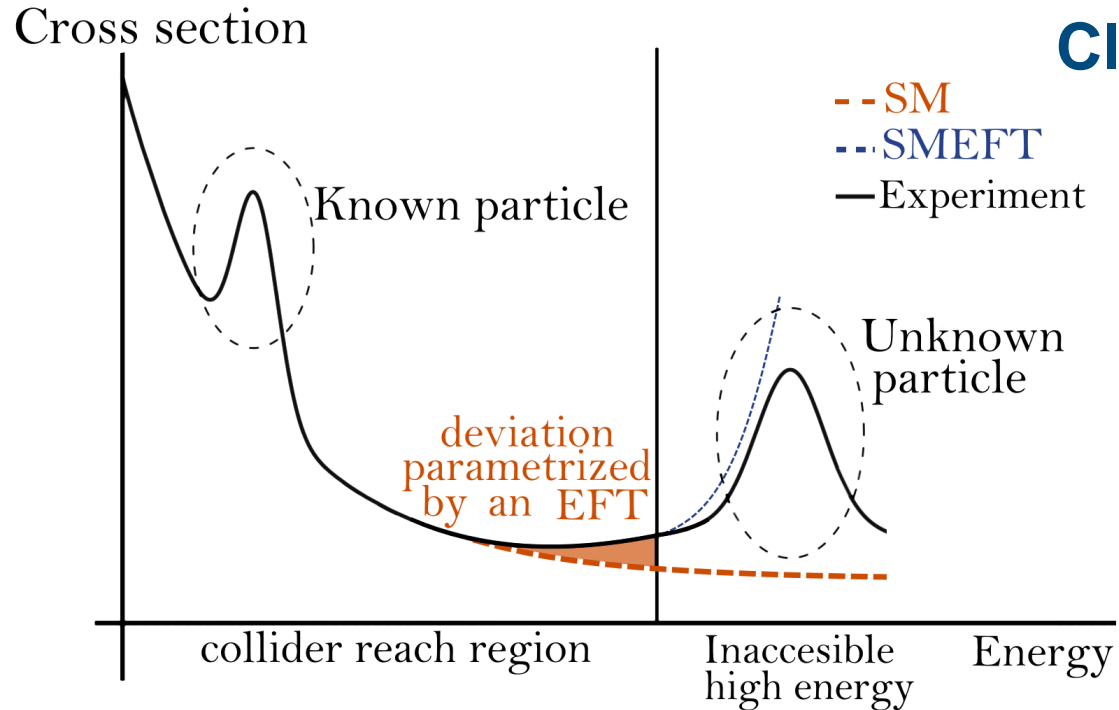


Tail hunting!

Original fig. by C. Severi, M. Thomas, E. Vryonidou

A trick of the tail

Precision with hadron colliders? Yes!



Clean channels + NP effects that grow with E



Tail hunting!

Heavy New Physics

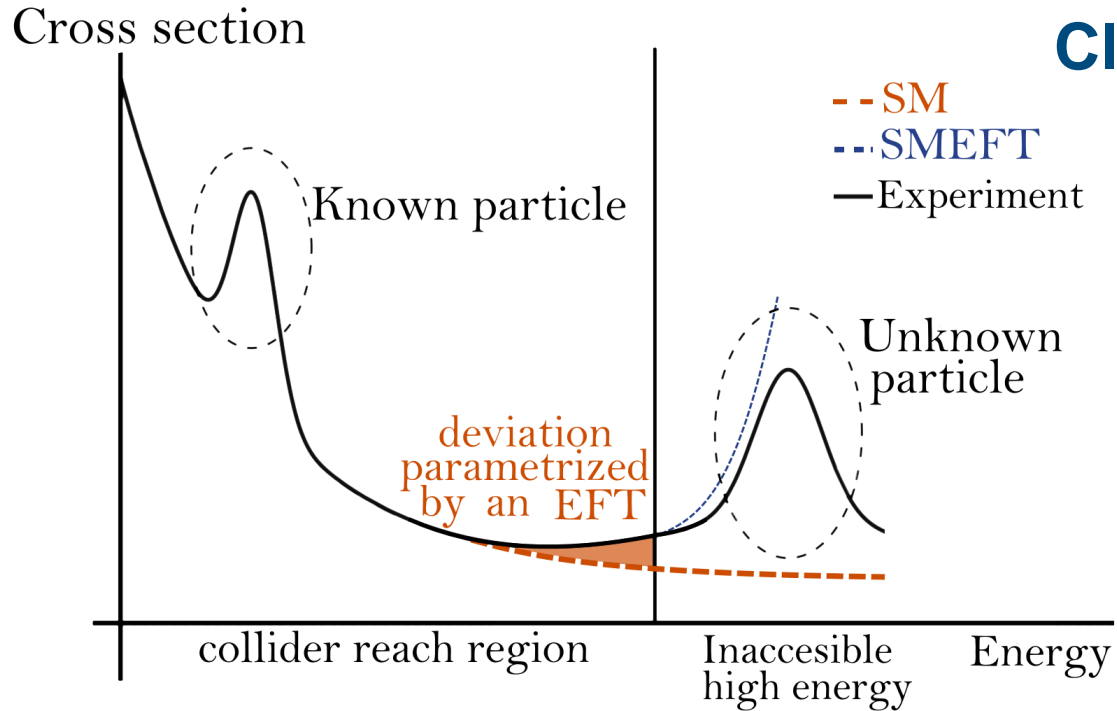


Effective Field Theories

Original fig. by C. Severi, M. Thomas, E. Vryonidou

A trick of the tail

Precision with hadron colliders? Yes!



Original fig. by C. Severi, M. Thomas, E. Vryonidou

Diboson processes offer a window into EW and Higgs dynamics.

Clean channels + NP effects that grow with E

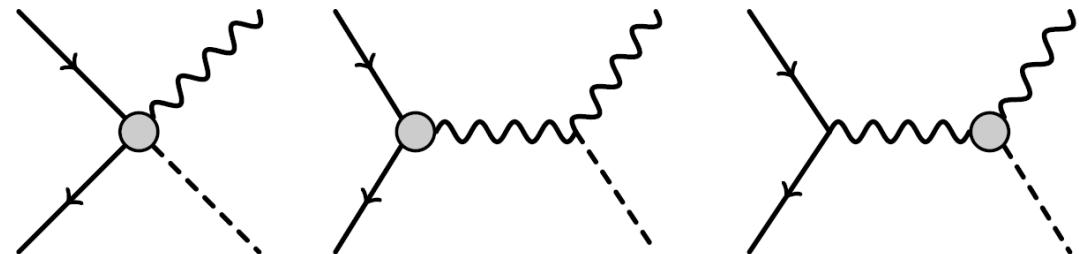


Tail hunting!

Heavy New Physics



Effective Field Theories



Standard Model EFT (SMEFT)

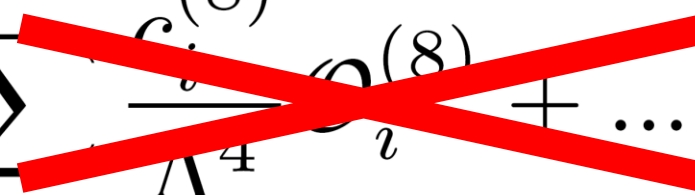
Standard Model EFT (SMEFT)

- Field content and gauge symmetries of the SM and linearly realized EWSB.

$$\mathcal{L} = \mathcal{L}_{SM} + \sum_i \frac{c_i^{(6)}}{\Lambda^2} \mathcal{O}_i^{(6)} + \sum_i \frac{c_i^{(8)}}{\Lambda^4} \mathcal{O}_i^{(8)} + \dots$$

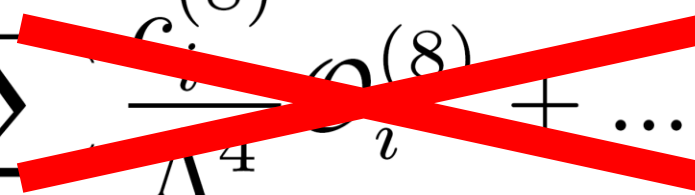
Standard Model EFT (SMEFT)

- Field content and gauge symmetries of the SM and linearly realized EWSB.

$$\mathcal{L} = \mathcal{L}_{SM} + \sum_i \frac{c_i^{(6)}}{\Lambda^2} \mathcal{O}_i^{(6)} + \sum_i \frac{c_i^{(8)}}{\Lambda^4} \mathcal{O}_i^{(8)} + \dots$$


Standard Model EFT (SMEFT)

- Field content and gauge symmetries of the SM and linearly realized EWSB.

$$\mathcal{L} = \mathcal{L}_{SM} + \sum_i \frac{c_i^{(6)}}{\Lambda^2} \mathcal{O}_i^{(6)} + \sum_i \frac{c_i^{(8)}}{\Lambda^4} \mathcal{O}_i^{(8)} + \dots$$


- Assume MFV and flavor universality.

For other flavour scen., see A.R., M. Thomas, E. Vryonidou arXiv:2306.09963

Standard Model EFT (SMEFT)


- Field content and gauge symmetries of the SM and linearly realized EWSB.

$$\mathcal{L} = \mathcal{L}_{SM} + \sum_i \frac{c_i^{(6)}}{\Lambda^2} \mathcal{O}_i^{(6)} + \sum_i \frac{c_i^{(8)}}{\Lambda^4} \mathcal{O}_i^{(8)} + \dots$$

- Assume MFV and flavor universality.

For other flavour scen., see A.R., M. Thomas, E. Vryonidou arXiv:2306.09963

$$\sigma = |\mathcal{M}_{SM}|^2 + 2\text{Re}(\mathcal{M}_{SM}\mathcal{M}_{BSM}^*) + |\mathcal{M}_{BSM}|^2$$



$$\underbrace{\propto c_i^{(6)}/\Lambda^2}_{\text{Interference}} \qquad \underbrace{\propto (c_i^{(6)}/\Lambda^2)^2}_{\text{BSM}}$$

Interference

New collider, new opportunities

$$pp \rightarrow W^{\pm} h$$

New collider, new opportunities

For $p_T^h > 550$ GeV:

$$pp \rightarrow W^\pm h$$

Higgs decay	Higgs BR	n_{HL-LHC}	n_{HE-LHC}	n_{FCC-hh}
$\bar{b}b$	$6 \cdot 10^{-1}$	10^3	10^4	10^5
$\tau\tau$	$6 \cdot 10^{-2}$	10^2	10^3	10^4
$\gamma\gamma$	$2 \cdot 10^{-3}$	10^0	10^2	10^3
$4l$	$2 \cdot 10^{-3}$	10^0	10^2	10^3
$\mu\mu$	$4 \cdot 10^{-4}$	10^0	10^1	10^2

New collider, new opportunities

For $p_T^h > 550$ GeV:

$$pp \rightarrow W^\pm h$$

	Higgs decay	Higgs BR	n_{HL-LHC}	n_{HE-LHC}	n_{FCC-hh}	
Today	$\bar{b}b$	$6 \cdot 10^{-1}$	10^3		10^5	$\frac{s}{\sqrt{s+b}} \ll 1$
	$\tau\tau$	$6 \cdot 10^{-2}$	10^2	10^3	10^4	
	$\gamma\gamma$	$2 \cdot 10^{-3}$	10^0	10^2	10^3	
	$4l$	$2 \cdot 10^{-3}$	10^0	10^2	10^3	
	$\mu\mu$	$4 \cdot 10^{-4}$	10^0	10^1	10^2	

New collider, new opportunities

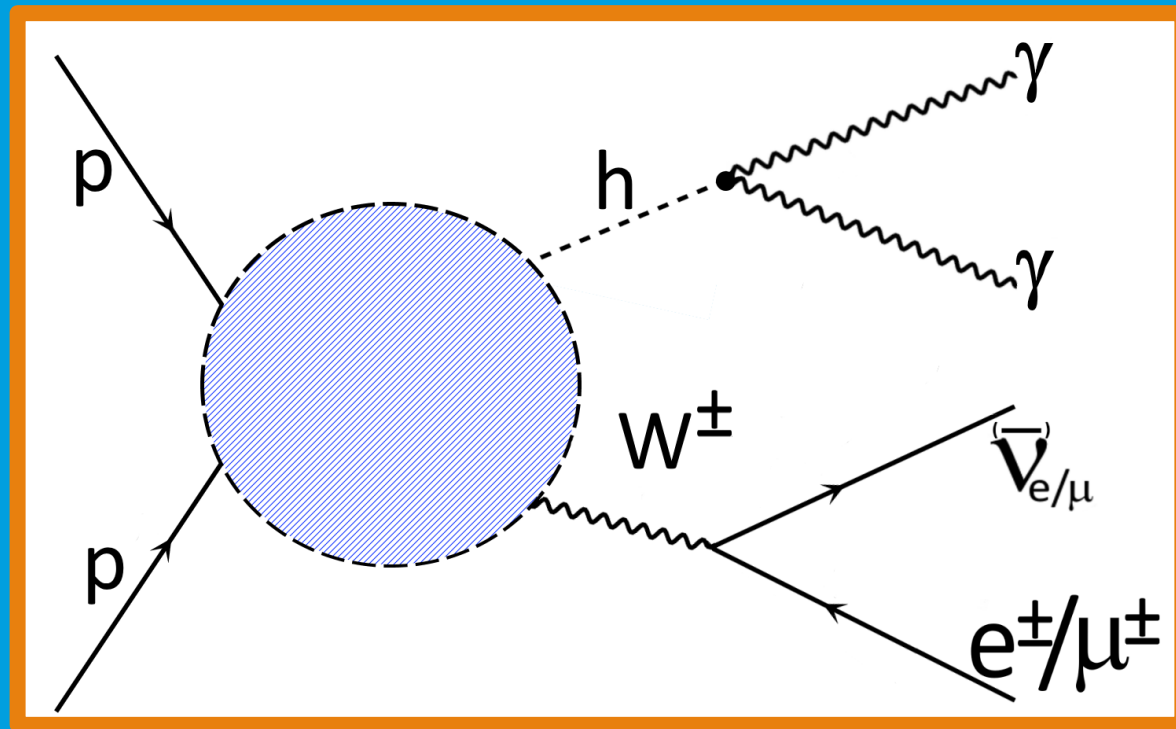
For $p_T^h > 550$ GeV:

$$pp \rightarrow W^\pm h$$

	Higgs decay	Higgs BR	n_{HL-LHC}	n_{HE-LHC}	n_{FCC-hh}	
Today	$\bar{b}b$	$6 \cdot 10^{-1}$	10^3		10^5	$\frac{s}{\sqrt{s+b}} \ll 1$
	$\tau\tau$	$6 \cdot 10^{-2}$	10^2	10^3	10^4	
Future	$\gamma\gamma$	$2 \cdot 10^{-3}$			10^3	$\frac{s}{\sqrt{s+b}} \approx 1$
	$4l$	$2 \cdot 10^{-3}$	10^0	10^2	10^3	
	$\mu\mu$	$4 \cdot 10^{-4}$	10^0	10^1	10^2	

Leptonic diphoton Wh.

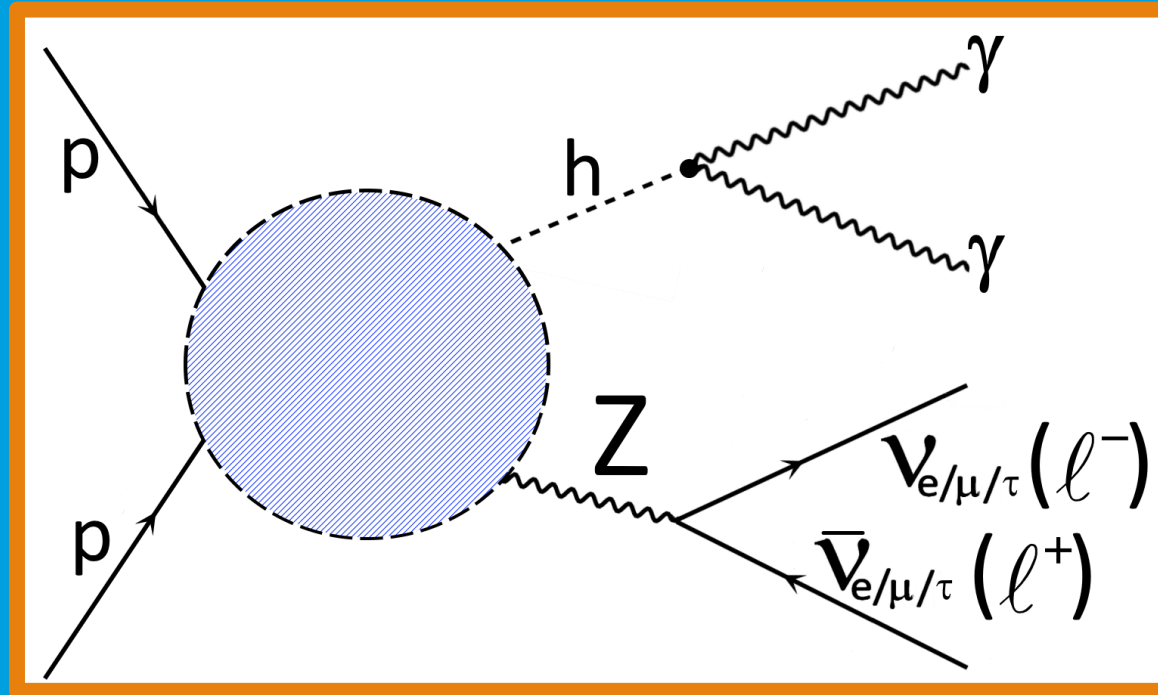
arXiv 2004.06122 (JHEP 07 (2020) 075)



$$pp \rightarrow W^\pm h \rightarrow l^\pm \nu \gamma \gamma$$

Diphoton Zh.

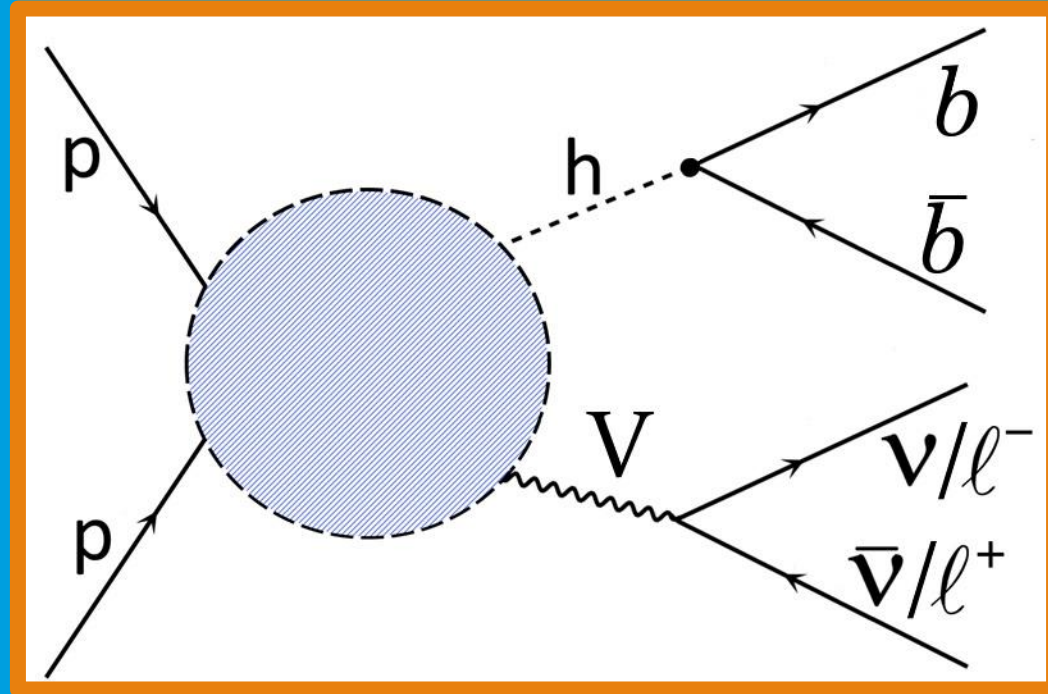
arXiv 2011.13941 (JHEP 04 (2021) 154)



$$pp \rightarrow Zh \rightarrow l^+ l^- (\nu \bar{\nu}) \gamma \gamma$$

Let them be quarks.

arXiv 2208.11134 (JHEP 06 (2023) 077)



$$pp \rightarrow V h \rightarrow \ell(\nu)\ell(\nu)b\bar{b}$$

Vh. What New Physics can we probe?

- In Warsaw basis

$$\mathcal{O}_{\varphi W} \quad \mathcal{O}_{\varphi \widetilde{W}} \quad \mathcal{O}_{\varphi q}^{(3)} \quad \mathcal{O}_{\varphi q}^{(1)} \quad \mathcal{O}_{\varphi d} \quad \mathcal{O}_{\varphi u}$$

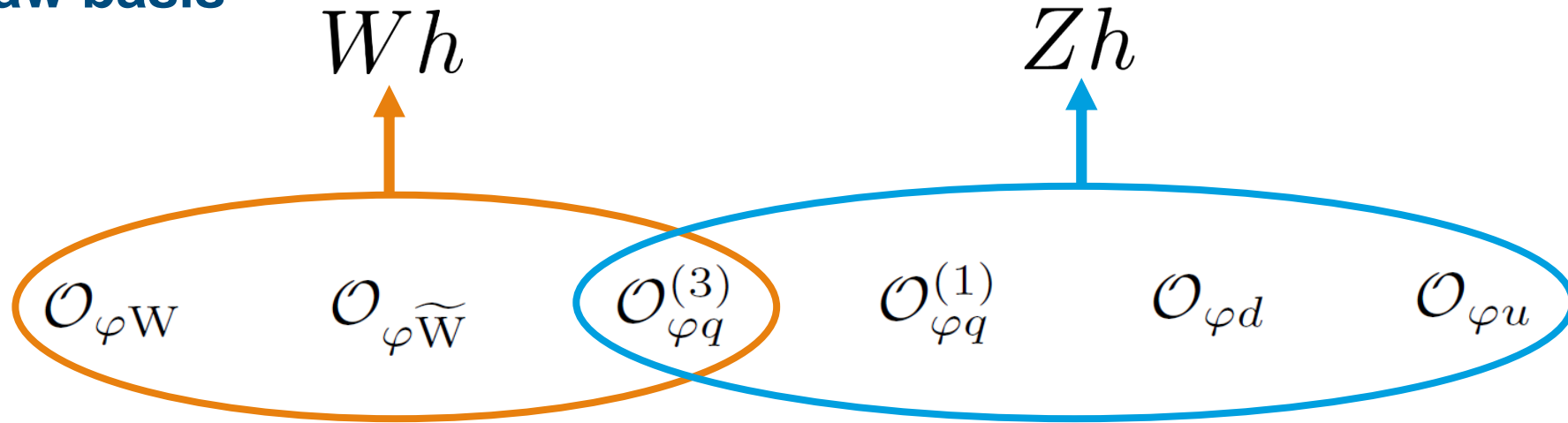
$$\mathcal{O}_{\varphi q}^{(3)} = (\bar{Q}_L \sigma^a \gamma^\mu Q_L) \left(i H^\dagger \sigma^a \overleftrightarrow{D}_\mu H \right), \quad \mathcal{O}_{\varphi q}^{(1)} = (\bar{Q}_L \gamma^\mu Q_L) \left(i H^\dagger \overleftrightarrow{D}_\mu H \right),$$

$$\mathcal{O}_{\varphi u} = (\bar{u}_R \gamma^\mu u_R) \left(i H^\dagger \overleftrightarrow{D}_\mu H \right), \quad \mathcal{O}_{\varphi d} = (\bar{d}_R \gamma^\mu d_R) \left(i H^\dagger \overleftrightarrow{D}_\mu H \right),$$

$$\mathcal{O}_{\varphi W} = H^\dagger H W^{a, \mu\nu} W_{\mu\nu}^a, \quad \mathcal{O}_{\varphi \widetilde{W}} = H^\dagger H W^{a, \mu\nu} \widetilde{W}_{\mu\nu}^a,$$

Vh. What New Physics can we probe?

- In Warsaw basis



$$\mathcal{O}_{\varphi q}^{(3)} = (\bar{Q}_L \sigma^a \gamma^\mu Q_L) \left(i H^\dagger \sigma^a \overleftrightarrow{D}_\mu H \right), \quad \mathcal{O}_{\varphi q}^{(1)} = (\bar{Q}_L \gamma^\mu Q_L) \left(i H^\dagger \overleftrightarrow{D}_\mu H \right),$$

$$\mathcal{O}_{\varphi u} = (\bar{u}_R \gamma^\mu u_R) \left(i H^\dagger \overleftrightarrow{D}_\mu H \right), \quad \mathcal{O}_{\varphi d} = (\bar{d}_R \gamma^\mu d_R) \left(i H^\dagger \overleftrightarrow{D}_\mu H \right),$$

$$\mathcal{O}_{\varphi W} = H^\dagger H W^{a, \mu\nu} W_{\mu\nu}^a, \quad \mathcal{O}_{\varphi \widetilde{W}} = H^\dagger H W^{a, \mu\nu} \widetilde{W}_{\mu\nu}^a,$$

High-energy behaviour

Amplitude level

V polarization	SM	$\mathcal{O}_{\varphi f}$	$\mathcal{O}_{\varphi W}$	$\mathcal{O}_{\varphi \tilde{W}}$
$\lambda = 0$	1	$\frac{\hat{s}}{\Lambda^2}$	$\frac{M_W^2}{\Lambda^2}$	0
$\lambda = \pm$	$\frac{M_W}{\sqrt{\hat{s}}}$	$\frac{\sqrt{\hat{s}} M_W}{\Lambda^2}$	$\frac{\sqrt{\hat{s}} M_W}{\Lambda^2}$	$\frac{\sqrt{\hat{s}} M_W}{\Lambda^2}$

High-energy behaviour

Amplitude level

V polarization	SM	$\mathcal{O}_{\varphi f}$	$\mathcal{O}_{\varphi W}$	$\mathcal{O}_{\varphi \widetilde{W}}$
$\lambda = 0$	1	$\frac{\hat{s}}{\Lambda^2}$	$\frac{M_W^2}{\Lambda^2}$	0
$\lambda = \pm$	$\frac{M_W}{\sqrt{\hat{s}}}$	$\frac{\sqrt{\hat{s}} M_W}{\Lambda^2}$	$\frac{\sqrt{\hat{s}} M_W}{\Lambda^2}$	$\frac{\sqrt{\hat{s}} M_W}{\Lambda^2}$

Cross section level

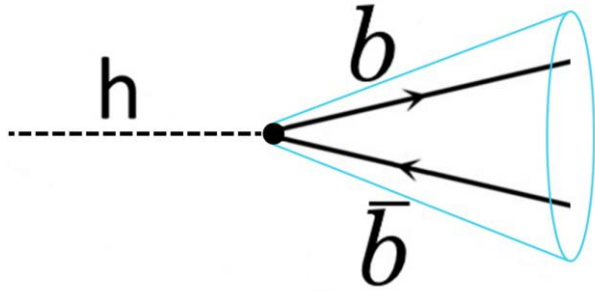
σ_{int}/σ_{SM}	p_T^h, p_T^V bins	
$\mathcal{O}_{\varphi f}$	$\sim \frac{\hat{s}}{\Lambda^2}$	
$\mathcal{O}_{\varphi W}$	$\sim \frac{m_W^2}{\Lambda^2}$	
$\mathcal{O}_{\varphi \widetilde{W}}$	$= 0$	

Differential in p_T  Only same polarization and CP interfere

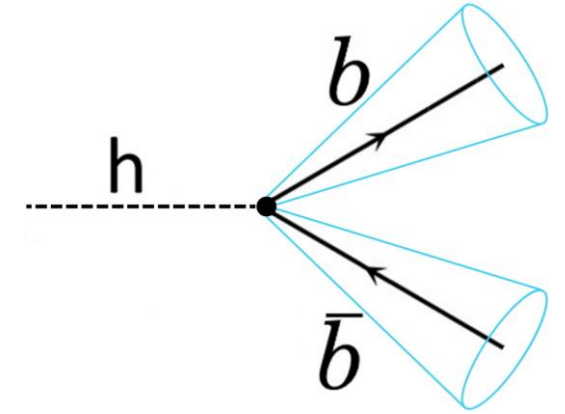
Vh.

Combining regimes in $h \rightarrow b\bar{b}$

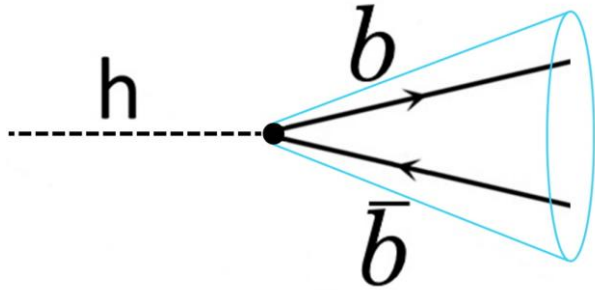
Boosted



Resolved



Boosted



ATLAS, 2008.02508

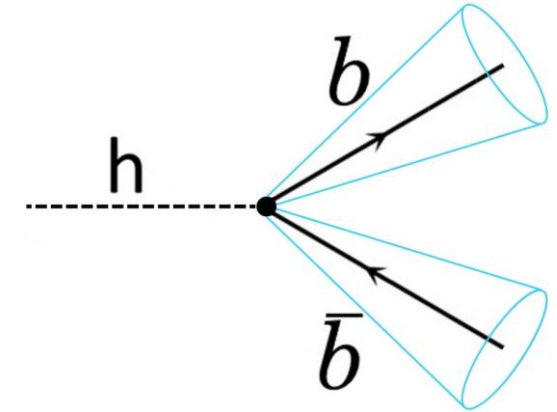
DOI: 10.1016/j.physletb.2021.136204

28th April 2021

Measurement of the associated production of a Higgs boson decaying into b -quarks with a vector boson at high transverse momentum in pp collisions at $\sqrt{s} = 13$ TeV with the ATLAS detector

The ATLAS Collaboration

Resolved



ATLAS, 2007.02873

DOI: 10.1140/epjc/s10052-020-08677-2

9th March 2021

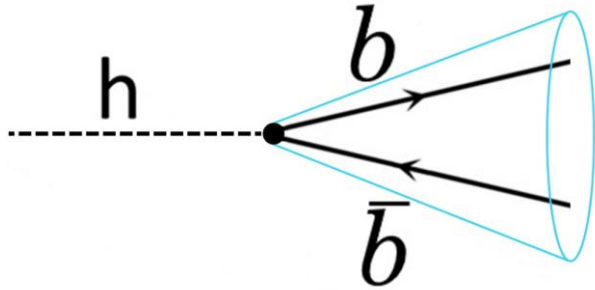
Measurements of WH and ZH production in the $H \rightarrow b\bar{b}$ decay channel in pp collisions at 13 TeV with the ATLAS detector

The ATLAS Collaboration

Vh.

Combining regimes in $h \rightarrow b\bar{b}$

Boosted



ATLAS, 2008.02508

DOI: 10.1016/j.physletb.2021.136204

28th April 2021

Measurement of the associated production of a Higgs boson decaying into b -quarks with a vector boson at high transverse momentum in pp collisions at $\sqrt{s} = 13$ TeV with the ATLAS detector

The ATLAS Collaboration

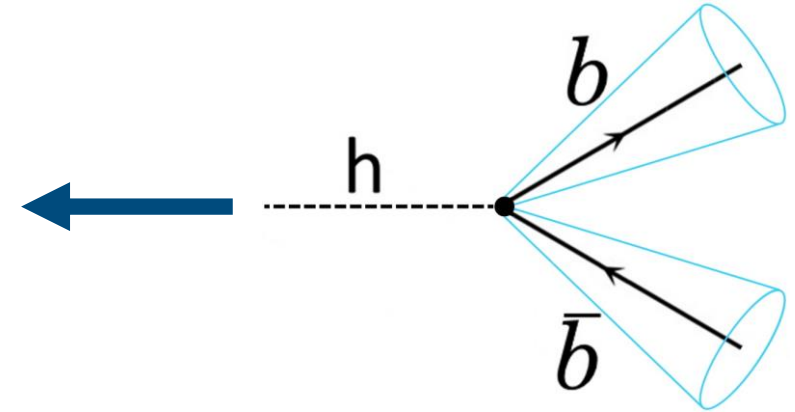
Scale-invariant tagging

Gouzevitch et al, 1303.6636
Bishara et al, 1611.03860

With use of
Mass-drop tagging

Butterworth et al, 0802.2470

Resolved



ATLAS, 2007.02873

DOI: 10.1140/epjc/s10052-020-08677-2

9th March 2021

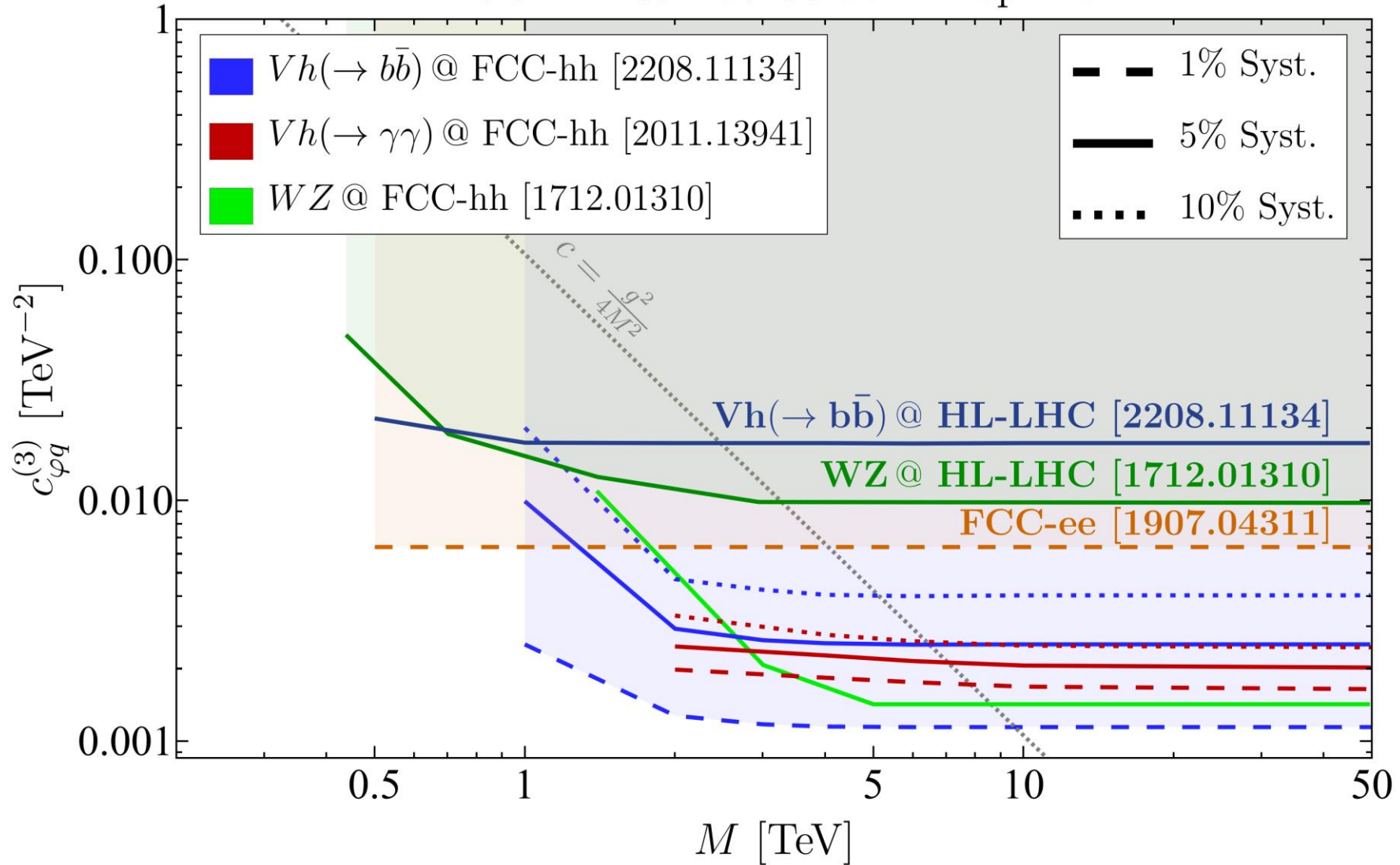
Measurements of WH and ZH production in the $H \rightarrow b\bar{b}$ decay channel in pp collisions at 13 TeV with the ATLAS detector

The ATLAS Collaboration

This strategy improves the bounds $\sim 7\%$ w.r.t. boosted-only at FCC-hh

95% C.L. on $c_{\varphi q}^{(3)}$

FCC-hh 100 TeV 30 ab^{-1} 1-op. fit.



Double binning.

Angular binning: a qualitative advantage.

Probing bosonic operators

Cross section level

σ_{int}/σ_{SM}	p_T^h, p_T^V bins	p_T^h, p_T^V and angular bins
$\mathcal{O}_{\varphi f}$	$\sim \frac{\hat{s}}{\Lambda^2}$	$\sim \frac{\hat{s}}{\Lambda^2}$
$\mathcal{O}_{\varphi W}$	$\sim \frac{m_W^2}{\Lambda^2}$	$\sim \frac{m_W^2}{\Lambda^2}$
$\mathcal{O}_{\varphi \tilde{W}}$	$= 0$	$\sim \frac{m_W \sqrt{\hat{s}}}{\Lambda^2}$

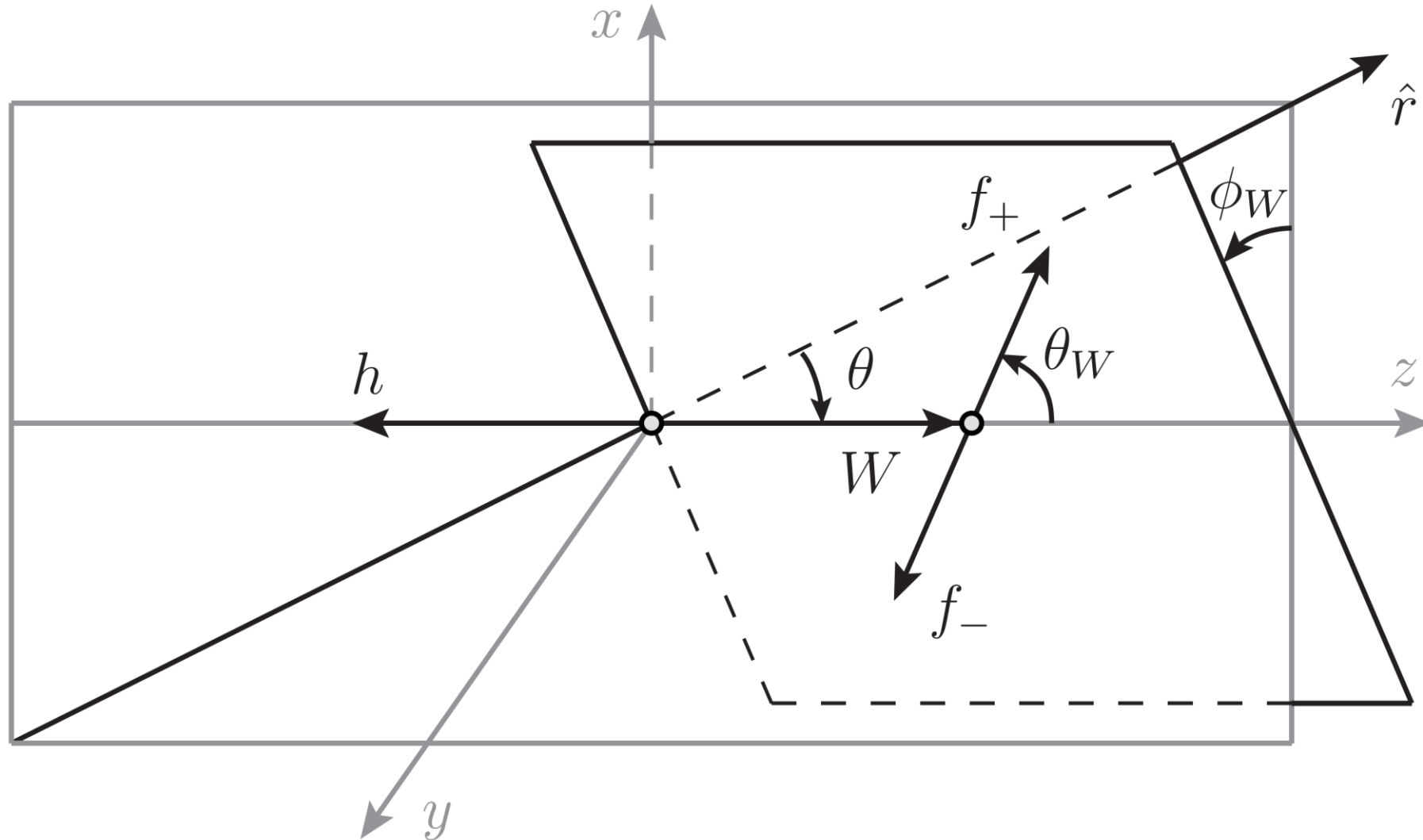
Differential in p_T and decay angles



Different polarizations and CP interfere

Interference patterns

Measuring angles resurrects interference



Wh. Angular binning for CP-odd operators

$$\sigma_{\mathcal{O}_{\varphi\widetilde{W}}}^{int} \sim \frac{\sqrt{\hat{s}}M_W}{\Lambda^2} \sin(\phi_W)$$

Wh. Angular binning for CP-odd operators

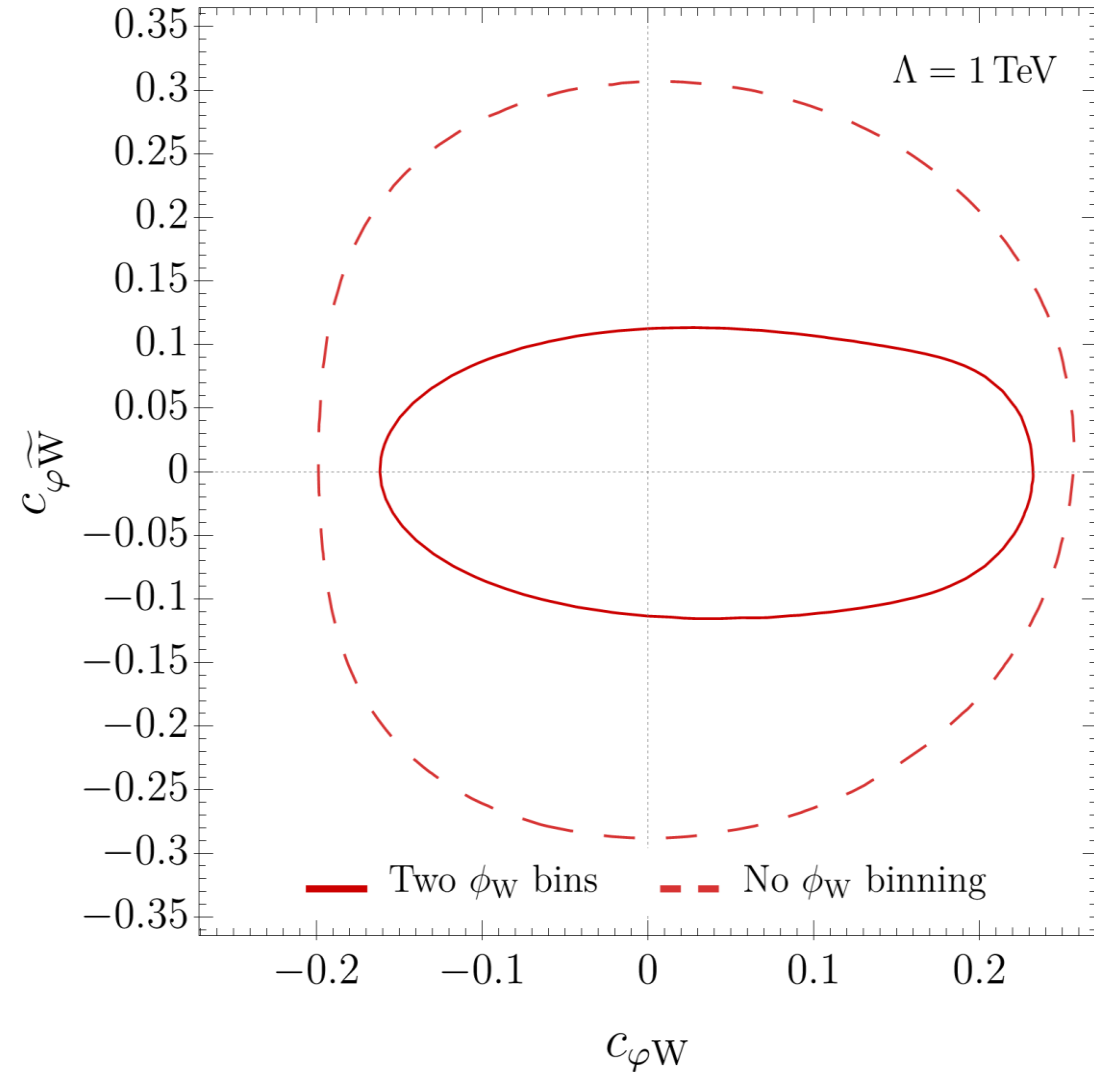
FCC-hh 100 TeV 30 ab⁻¹, 5% Syst.

Differential in p_T^h and ϕ_W

$$\sigma_{\mathcal{O}_{\phi\widetilde{W}}}^{int} \sim \frac{\sqrt{\hat{s}} M_W}{\Lambda^2} \sin(\phi_W)$$

$$p_T^h \in \{200, 400, 600, 800, 1000, \infty\} \text{ GeV}$$

$$\phi_W \in [-\pi, 0], [0, \pi]$$



Zh. Rapidity binning to lift cancellations

$$\sigma_{\varphi q}^{int(1)} \propto s_W^2 Q - T_3$$

Cancellation of up and down contributions

Zh. Rapidity binning to lift cancellations

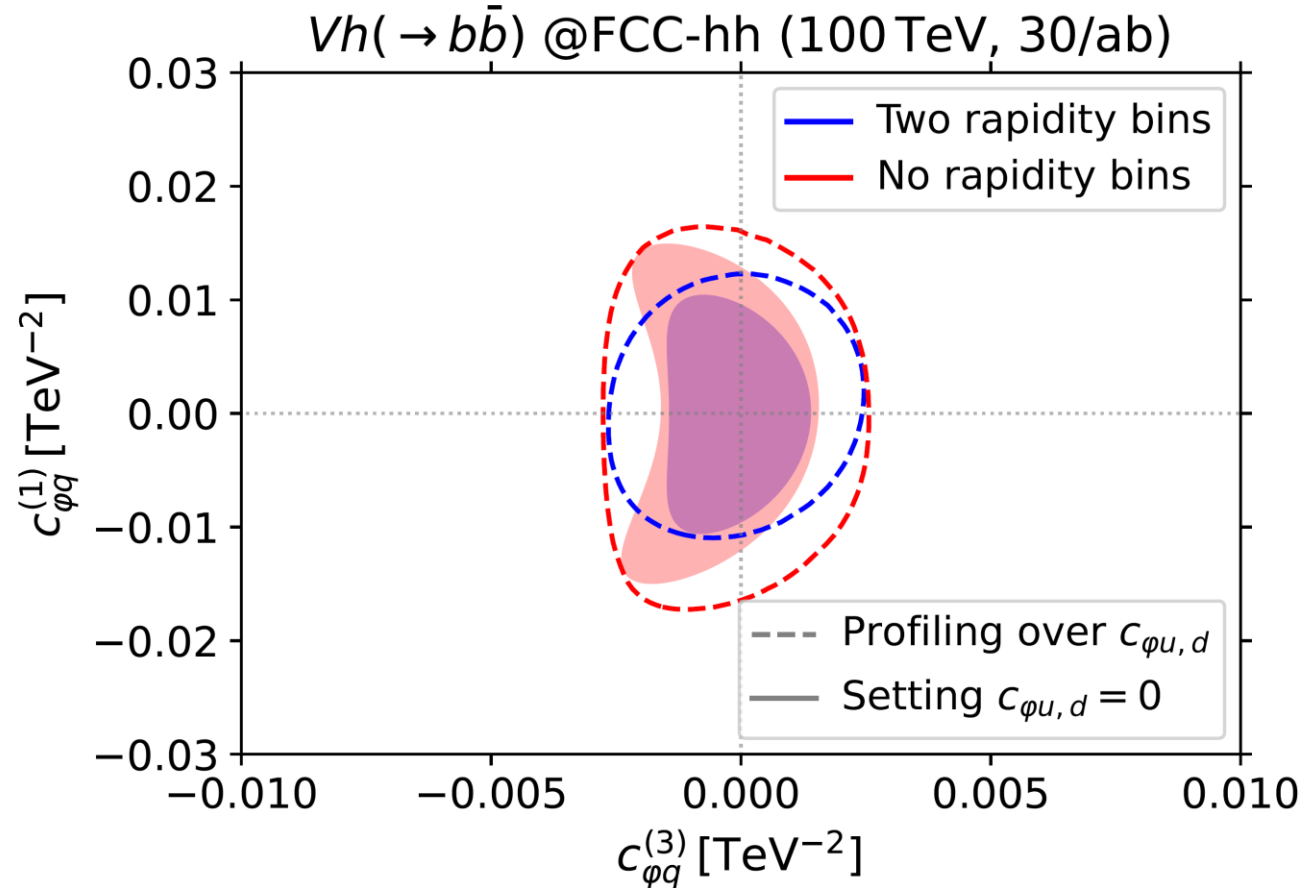
$$\sigma_{\mathcal{O}_{\varphi q}^{(1)}}^{int} \propto s_W^2 Q - T_3$$

Cancellation of up and down contributions

$$\text{Min}\{p_T^h, p_T^Z\} \in \{200, 400, 600, 800, 1000, \infty\} \text{ GeV}$$

$$|y_{Zh}| \in [0, 2), [2, 6]$$

(Slightly different rapidity binning for $Z \rightarrow \nu\bar{\nu}$)



Significant impact on $\mathcal{O}_{\varphi q}^{(1)}$ due to the lift of the cancellation.

Exploiting complementarity.

A showcase for the full diboson and FCC programs.

$$c_{\varphi q}^{(3)} = + \frac{\Lambda^2}{4m_W^2} g^2 (\delta g_L^{Zu} - \delta g_L^{Zd} - c_W^2 \delta g_{1z})$$

$$c_{\varphi q}^{(1)} = - \frac{\Lambda^2}{4m_W^2} g^2 \left(\delta g_L^{Zu} + \delta g_L^{Zd} + \frac{1}{3} (t_W^2 \delta \kappa_\gamma - s_W^2 \delta g_{1z}) \right)$$

$$c_{\varphi u} = - \frac{\Lambda^2}{2m_W^2} g^2 \left(\delta g_R^{Zu} + \frac{2}{3} (t_W^2 \delta \kappa_\gamma - s_W^2 \delta g_{1z}) \right)$$

$$c_{\varphi d} = - \frac{\Lambda^2}{2m_W^2} g^2 \left(\delta g_R^{Zd} - \frac{1}{3} (t_W^2 \delta \kappa_\gamma - s_W^2 \delta g_{1z}) \right)$$

$$\begin{aligned} \mathcal{L}_{TGC} \supset & ie (1 + \delta \kappa_\gamma) A^{\mu\nu} W_\mu^+ W_\nu^- \\ & + ig c_W (1 + \delta g_{1z}) (W_{\mu\nu}^+ W^{-,\mu} - W_{\mu\nu}^- W^{+,\mu}) Z^\nu \end{aligned}$$

FCC-hh 100 TeV 30 ab⁻¹, 95% C.L., 5% Syst.

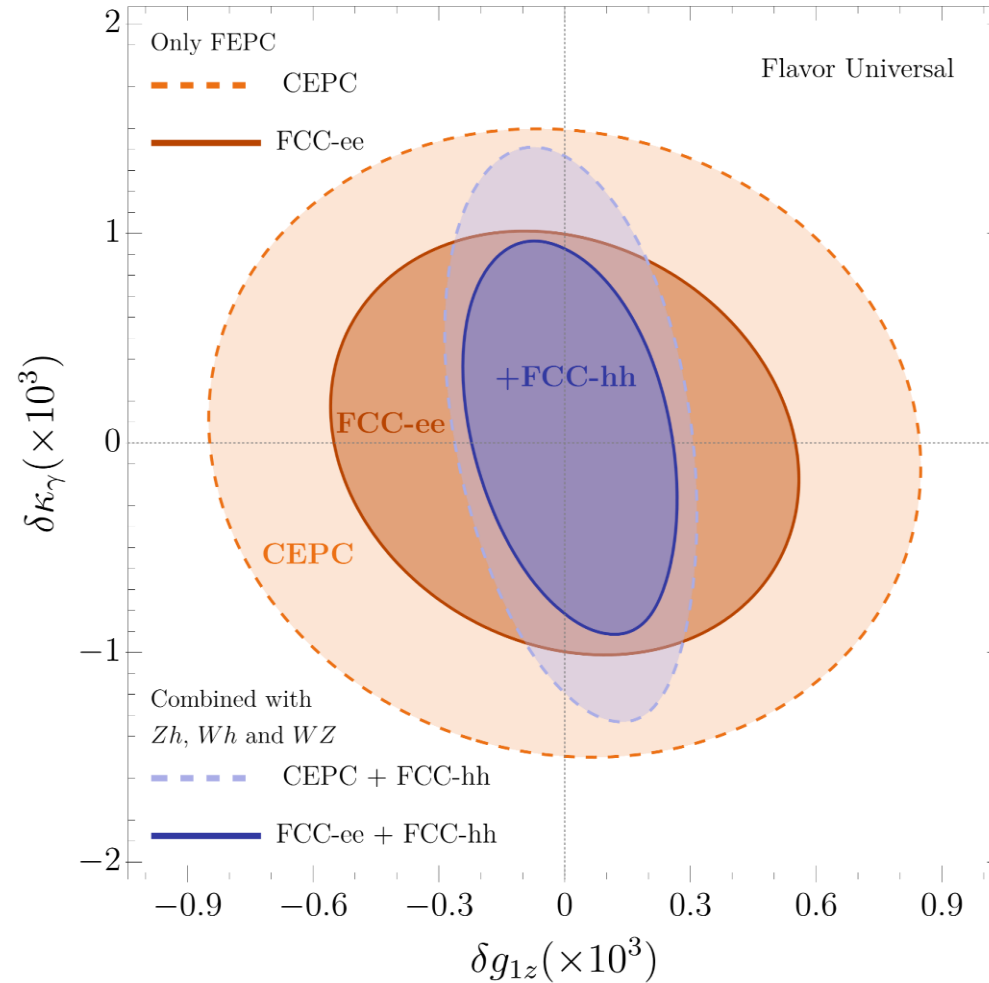
$$c_{\varphi q}^{(3)} = + \frac{\Lambda^2}{4m_W^2} g^2 (\delta g_L^{Zu} - \delta g_L^{Zd} - c_W^2 \delta g_{1z})$$

$$c_{\varphi q}^{(1)} = - \frac{\Lambda^2}{4m_W^2} g^2 \left(\delta g_L^{Zu} + \delta g_L^{Zd} + \frac{1}{3} (t_W^2 \delta \kappa_\gamma - s_W^2 \delta g_{1z}) \right)$$

$$c_{\varphi u} = - \frac{\Lambda^2}{2m_W^2} g^2 \left(\delta g_R^{Zu} + \frac{2}{3} (t_W^2 \delta \kappa_\gamma - s_W^2 \delta g_{1z}) \right)$$

$$c_{\varphi d} = - \frac{\Lambda^2}{2m_W^2} g^2 \left(\delta g_R^{Zd} - \frac{1}{3} (t_W^2 \delta \kappa_\gamma - s_W^2 \delta g_{1z}) \right)$$

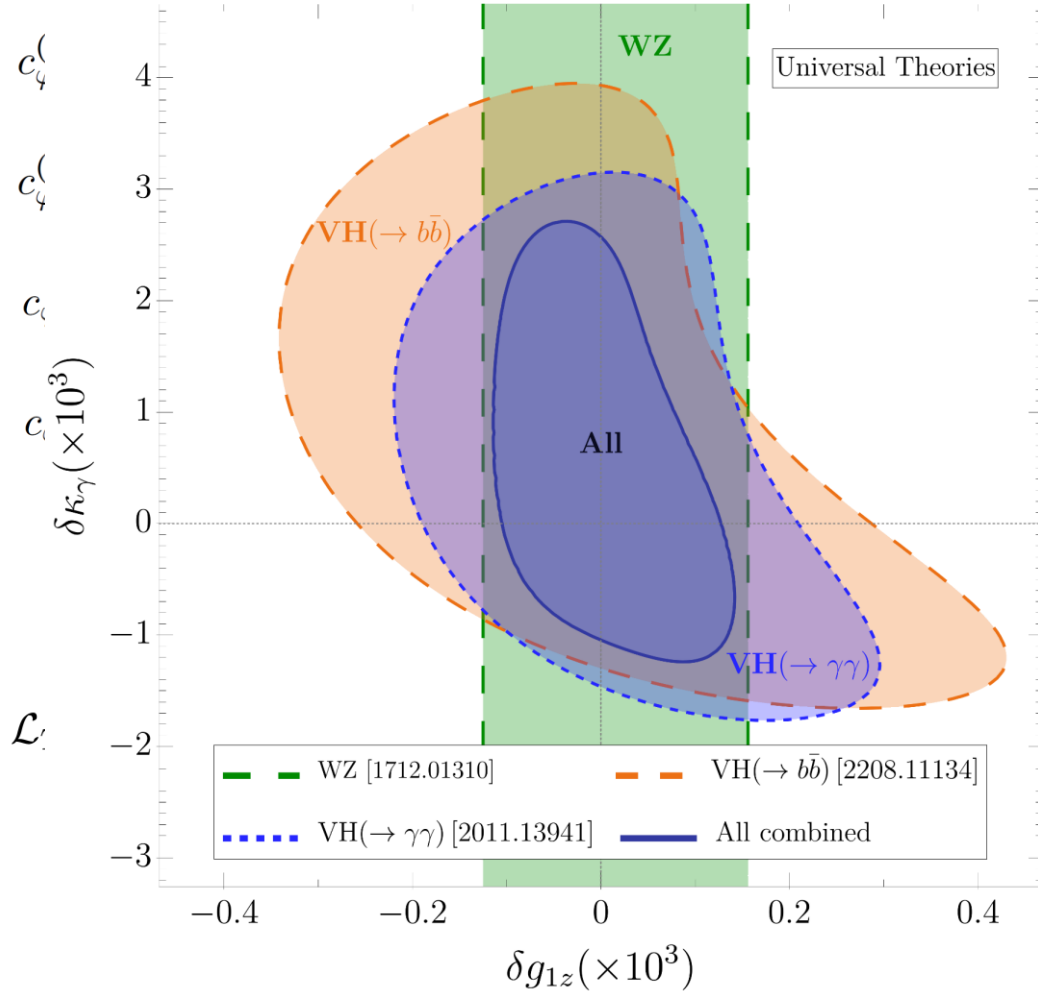
$$\mathcal{L}_{TGC} \supset ie (1 + \delta \kappa_\gamma) A^{\mu\nu} W_\mu^+ W_\nu^- + ig c_W (1 + \delta g_{1z}) (W_{\mu\nu}^+ W^{-,\mu} - W_{\mu\nu}^- W^{+,\mu}) Z^\nu$$



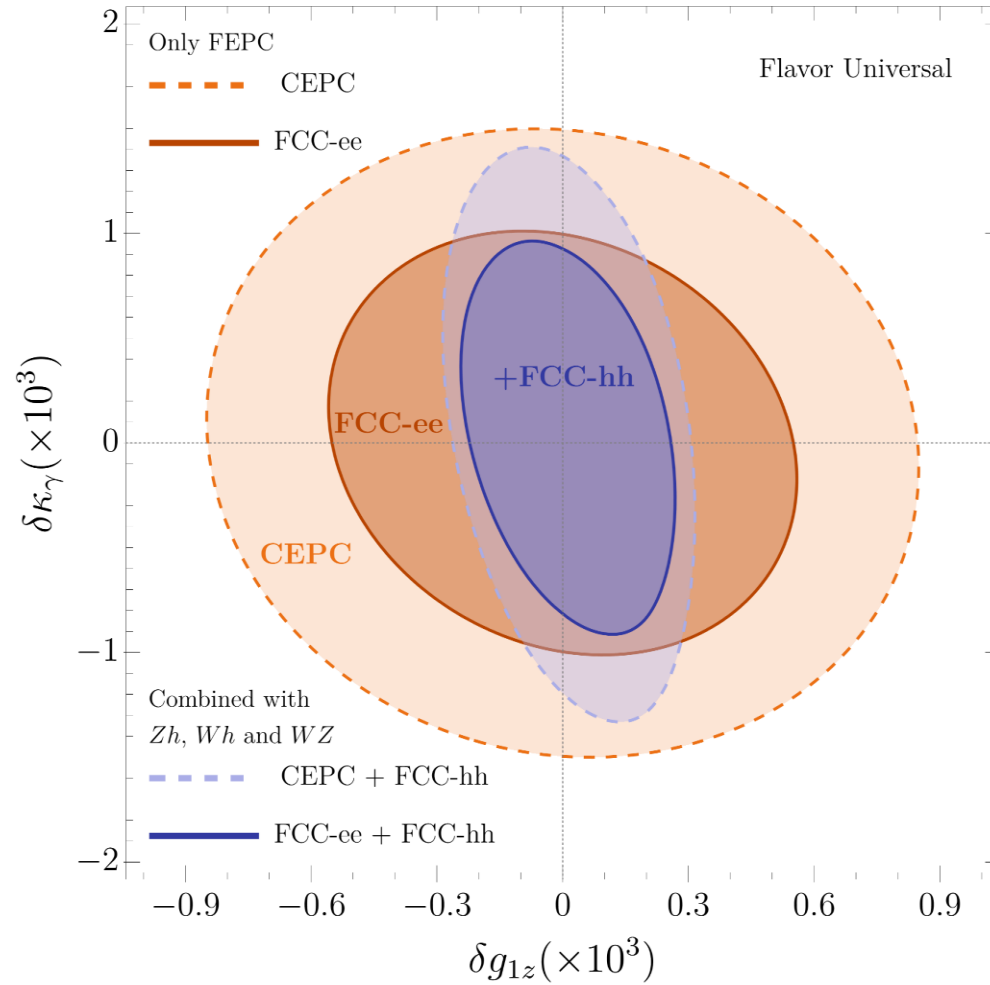
Complementarity with future lepton colliders

Impact on aTGC bounds

FCC-hh 100 TeV 30 ab⁻¹, 95% C.L., 5% Syst.



FCC-hh 100 TeV 30 ab⁻¹, 95% C.L., 5% Syst.



Complementarity among diboson processes

Conclusions

- $(W, Z) h$ probes several operators.
- A simple p_T binning yields competitive sensitivity to $\mathcal{O}_{\varphi q}^{(3)}$.
- $h \rightarrow \gamma\gamma$ will become available at FCC-hh, opening new possibilities.
- $h \rightarrow \gamma\gamma$ and $h \rightarrow b\bar{b}$ achieve similar results in different ways.
- In Wh , a binning in ϕ_W gives an observable linear in $\mathcal{O}_{\varphi\widetilde{W}}$.
- In Zh , a binning in rapidity improves the sensitivity to $\mathcal{O}_{\varphi q}^{(1)}$.
- Wh and Zh with are not exploration channels, but important to probe different directions.

Thank you for your attention

Contact



The University of Manchester

www.manchester.ac.uk

Alejo N. Rossia

HEP Theory Group – Dept. Of Physics and Astronomy

E-mail: alejo dot rossia at manchester dot ac dot uk

<http://www.hep.man.ac.uk/>

Appendix.

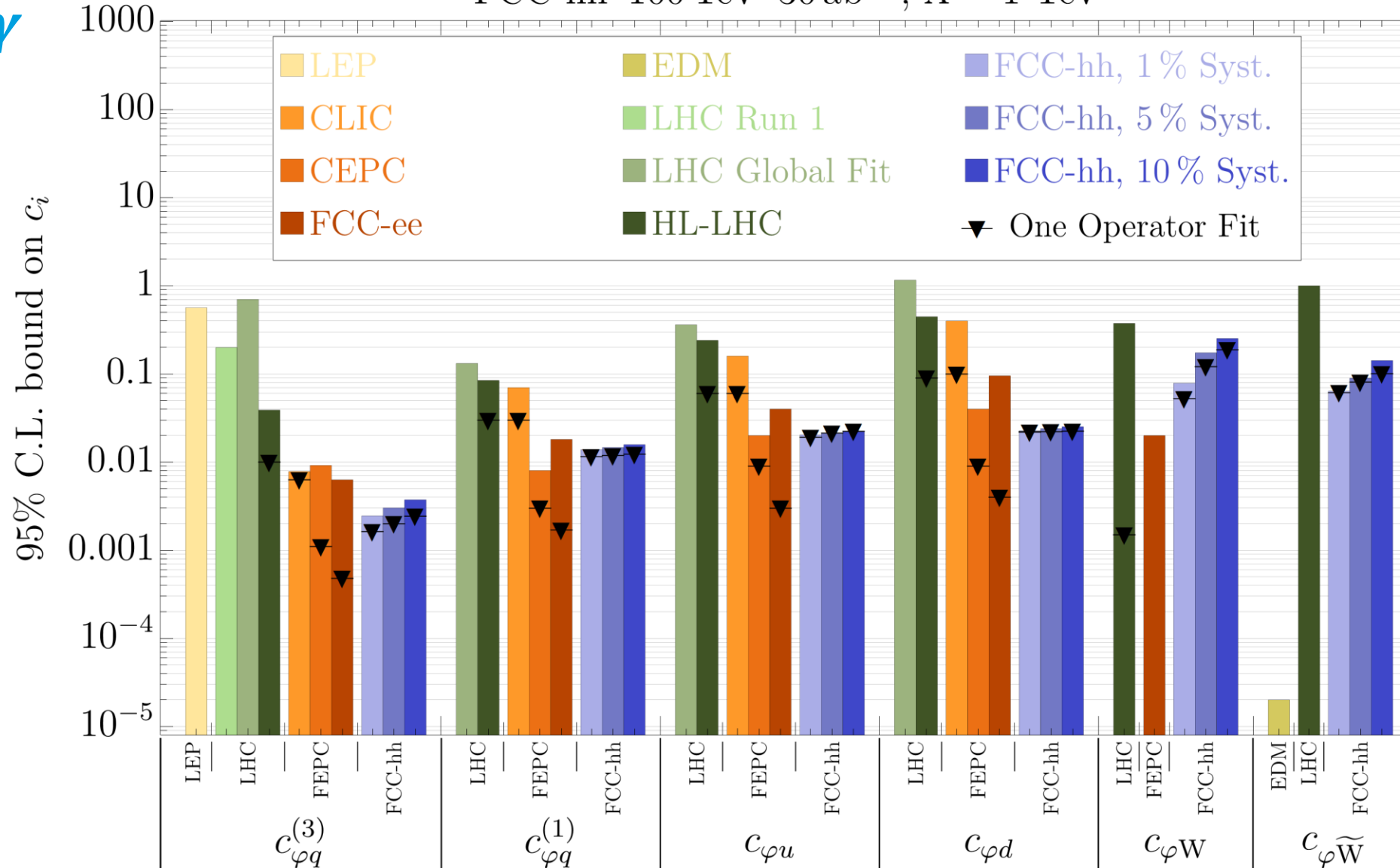
For even more details, read our papers or contact us.

Vh.

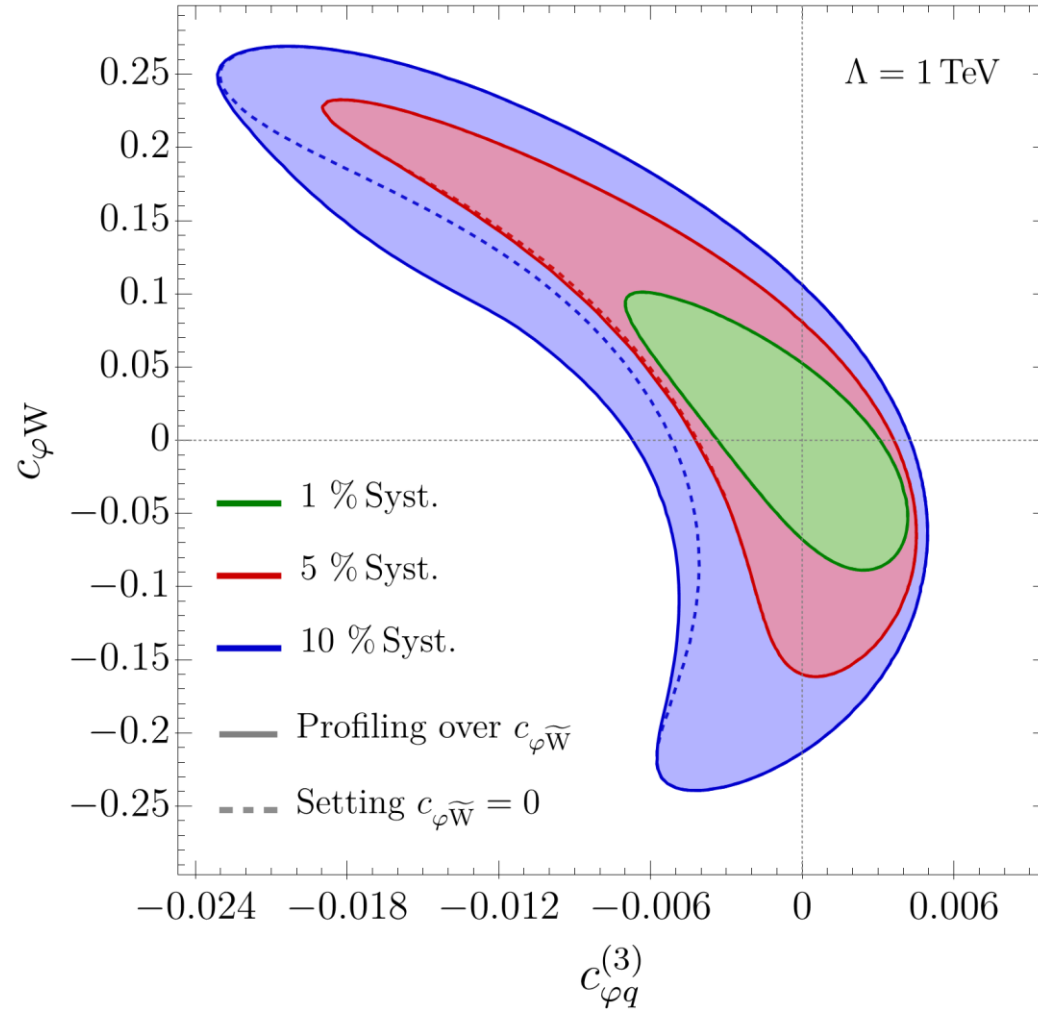
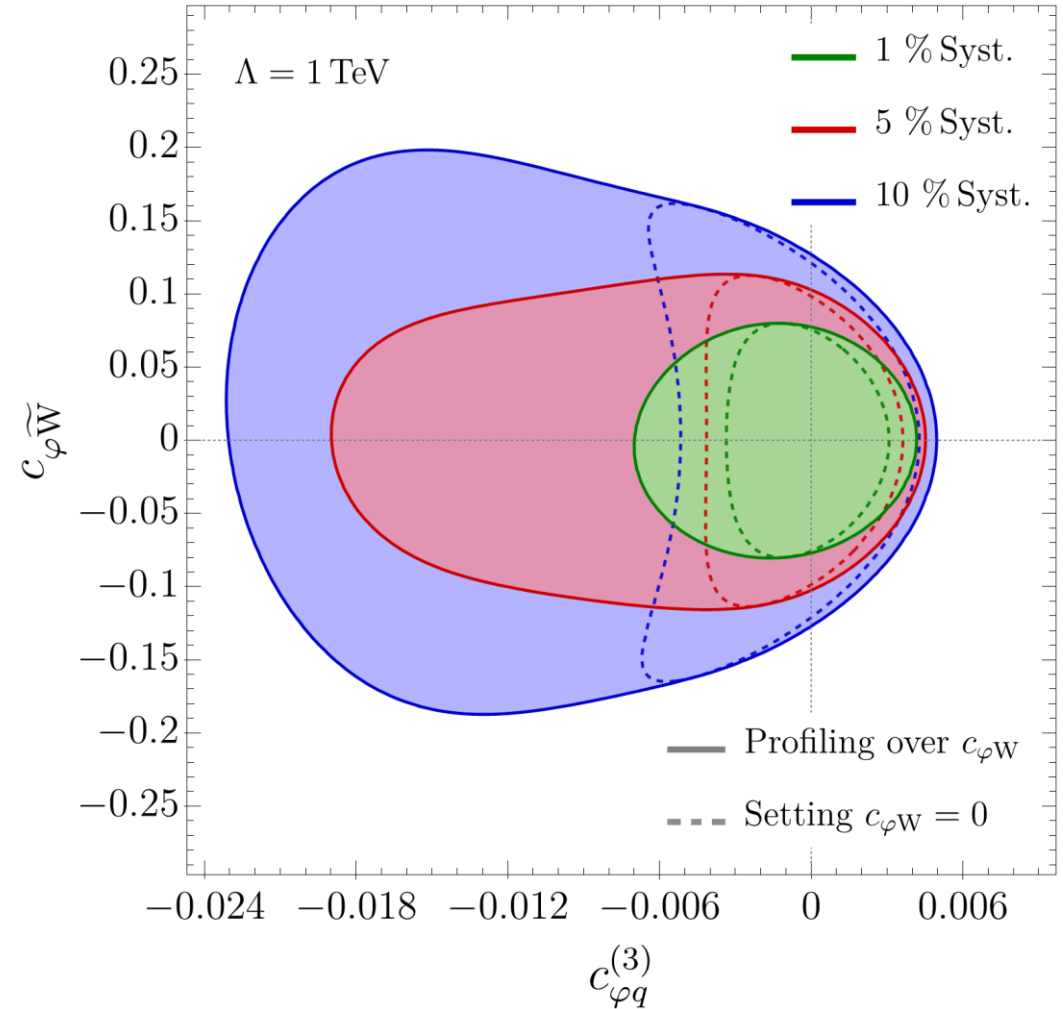
Comparing our bounds with other colliders

$h \rightarrow \gamma\gamma$

FCC-hh 100 TeV 30 ab⁻¹, $\Lambda = 1$ TeV

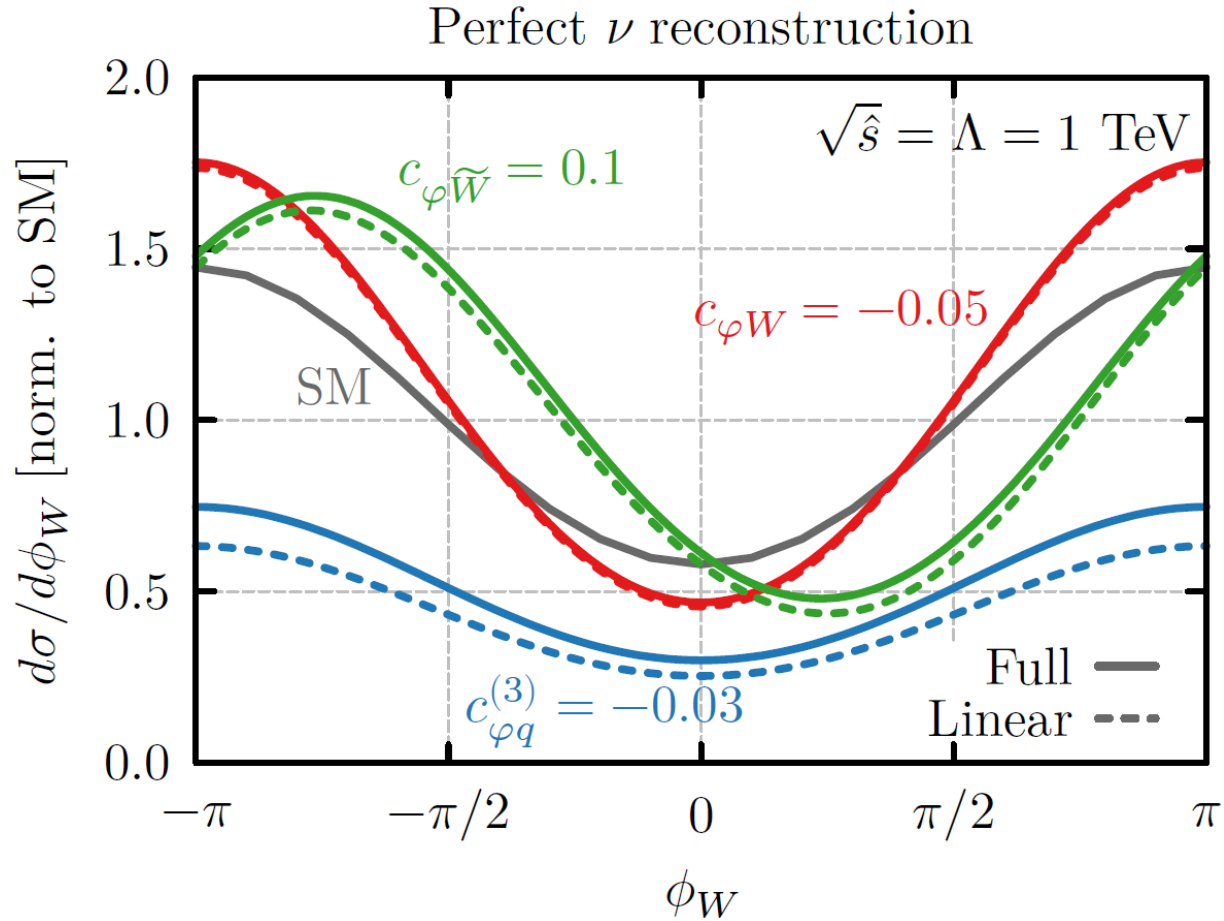


- 95% CL bounds

FCC-hh 100 TeV 30 ab⁻¹FCC-hh 100 TeV 30 ab⁻¹

Wh.

Interference patterns



Differential in p_T^h and ϕ_W

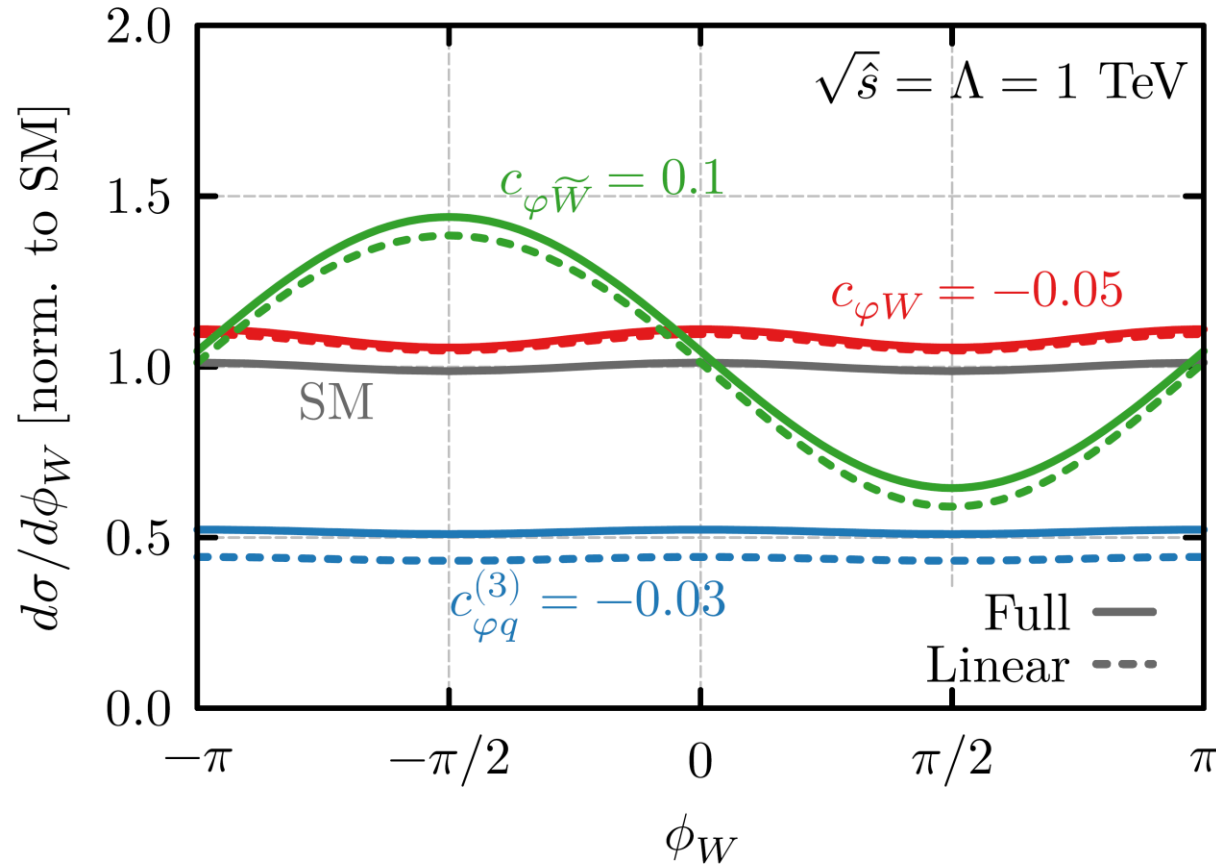
$$\sigma_{\mathcal{O}_{\phi q}^{(3)}}^{int} \sim \frac{\hat{s}}{\Lambda^2}$$

$$\sigma_{\mathcal{O}_{\phi W}}^{int} \sim \frac{\sqrt{\hat{s}} M_W}{\Lambda^2} \cos(\phi_W)$$

$$\sigma_{\mathcal{O}_{\phi\tilde{W}}}^{int} \sim \frac{\sqrt{\hat{s}} M_W}{\Lambda^2} \sin(\phi_W)$$

$$p_T^h \in \{200, 400, 600, 800, 1000, \infty\} \text{ GeV}$$

$$\phi_W \in [-\pi, 0], [0, \pi]$$

With ν reconstruction ambiguityDifferential in p_T^h and ϕ_W

$$\sigma_{\mathcal{O}_{\phi q}^{(3)}}^{int} \sim \frac{\hat{s}}{\Lambda^2} \quad \nu \text{ reconstruction}$$

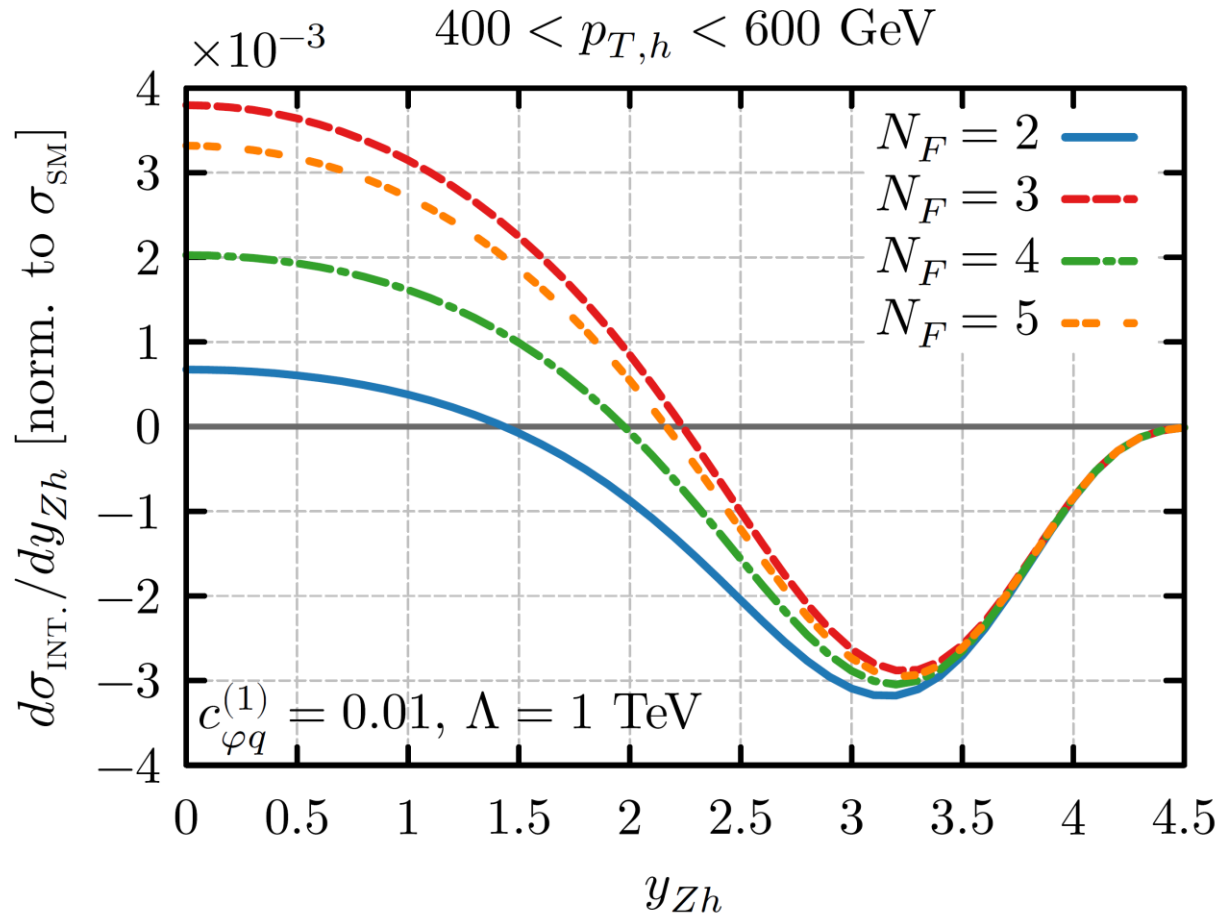
$$(\phi_W \rightarrow \pi - \phi_W)$$

$$\sigma_{\mathcal{O}_{\phi W}}^{int} \sim \frac{\sqrt{\hat{s}} M_W}{\Lambda^2} \cos(\phi_W)$$

$$\sigma_{\mathcal{O}_{\phi\tilde{W}}}^{int} \sim \frac{\sqrt{\hat{s}} M_W}{\Lambda^2} \sin(\phi_W)$$

$$p_T^h \in \{200, 400, 600, 800, 1000, \infty\} \text{ GeV}$$

$$\phi_W \in [-\pi, 0], [0, \pi]$$



$$\sigma_{\mathcal{O}_{\varphi q}^{(1)}}^{int} \propto s_W^2 Q - T_3$$

Cancellation of up and down contributions

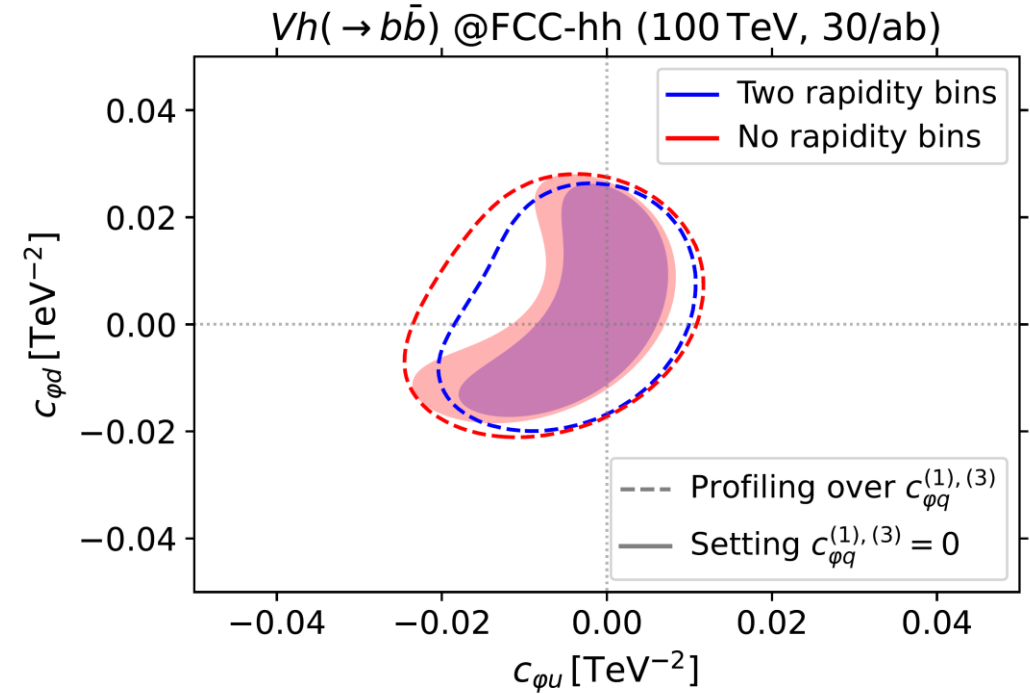
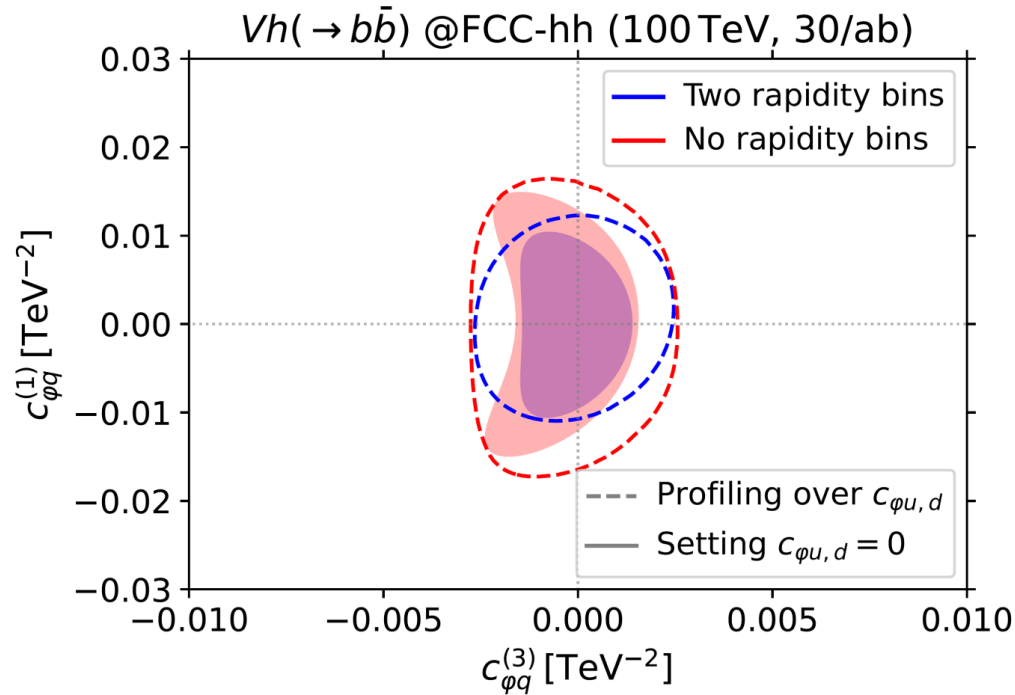
Differential in p_T and rapidity

$$\text{Min}\{p_T^h, p_T^Z\} \in \{200, 400, 600, 800, 1000, \infty\} \text{ GeV}$$

$$|y_{Zh}| \in [0, 2), [2, 6]$$

(Slightly different rapidity binning for $Z \rightarrow \nu\bar{\nu}$)

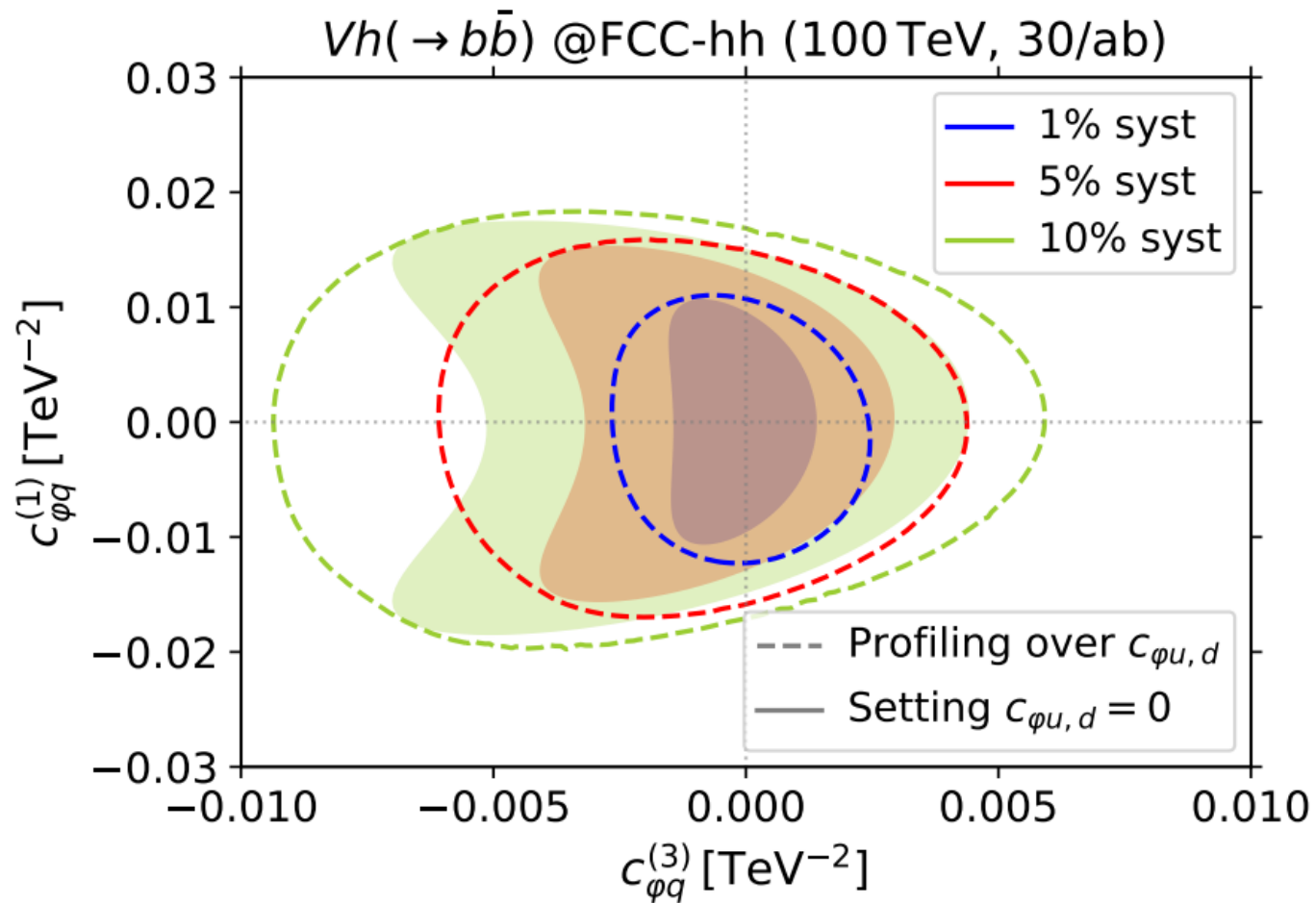
Rapidity binning effects



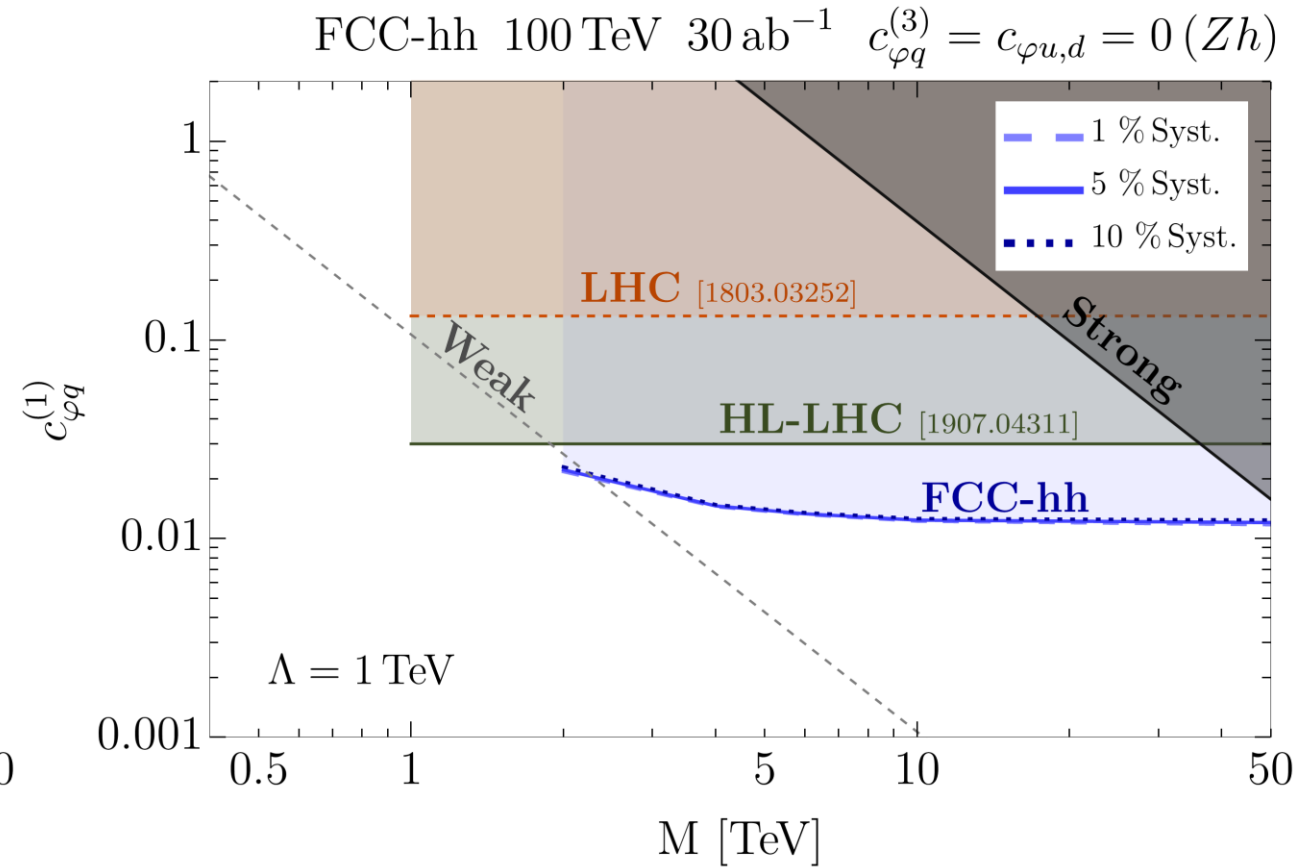
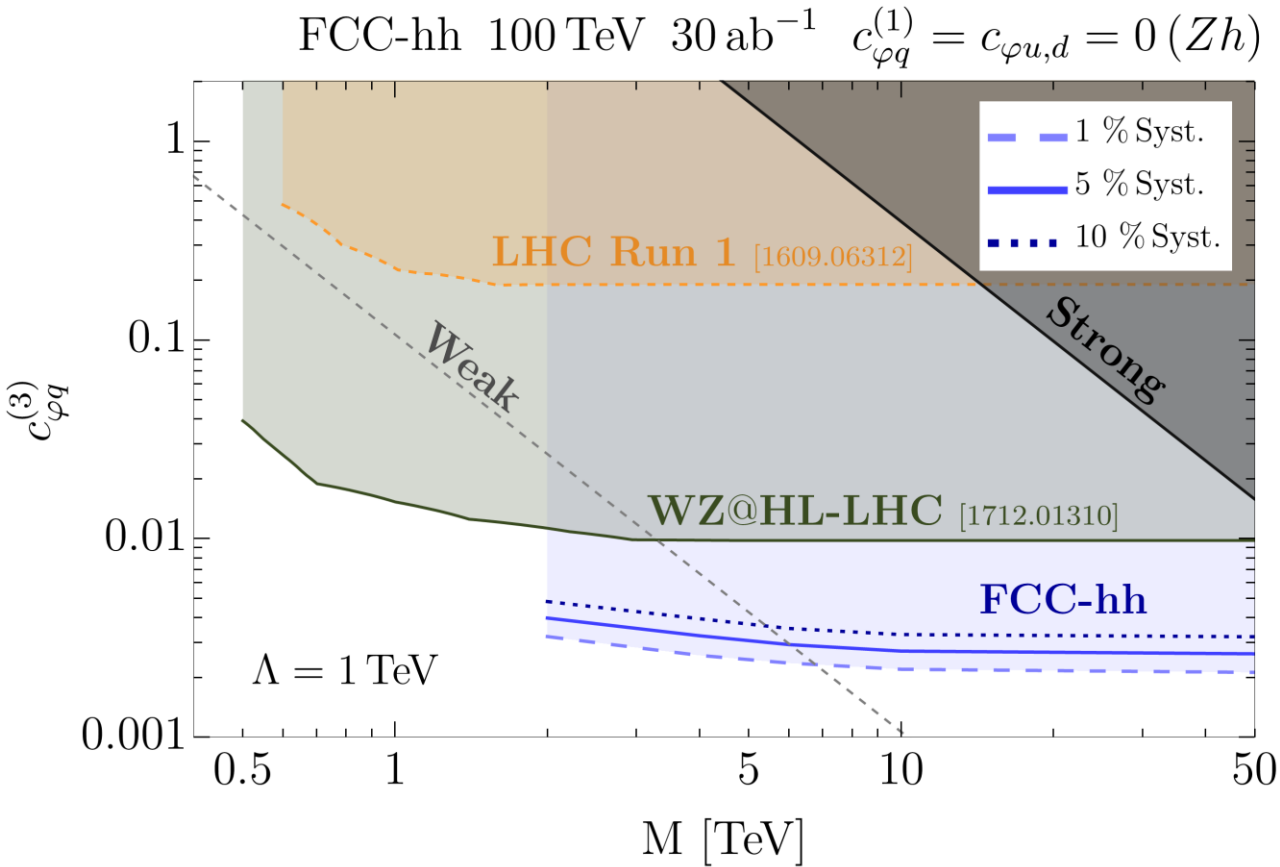
Significant impact on $\mathcal{O}_{\phi q}^{(1)}$ due to the lift of the cancellation.

Reduces the correlation between $\mathcal{O}_{\phi u}$ and $\mathcal{O}_{\phi d}$.

More results



- 95% CL bounds



Vh.

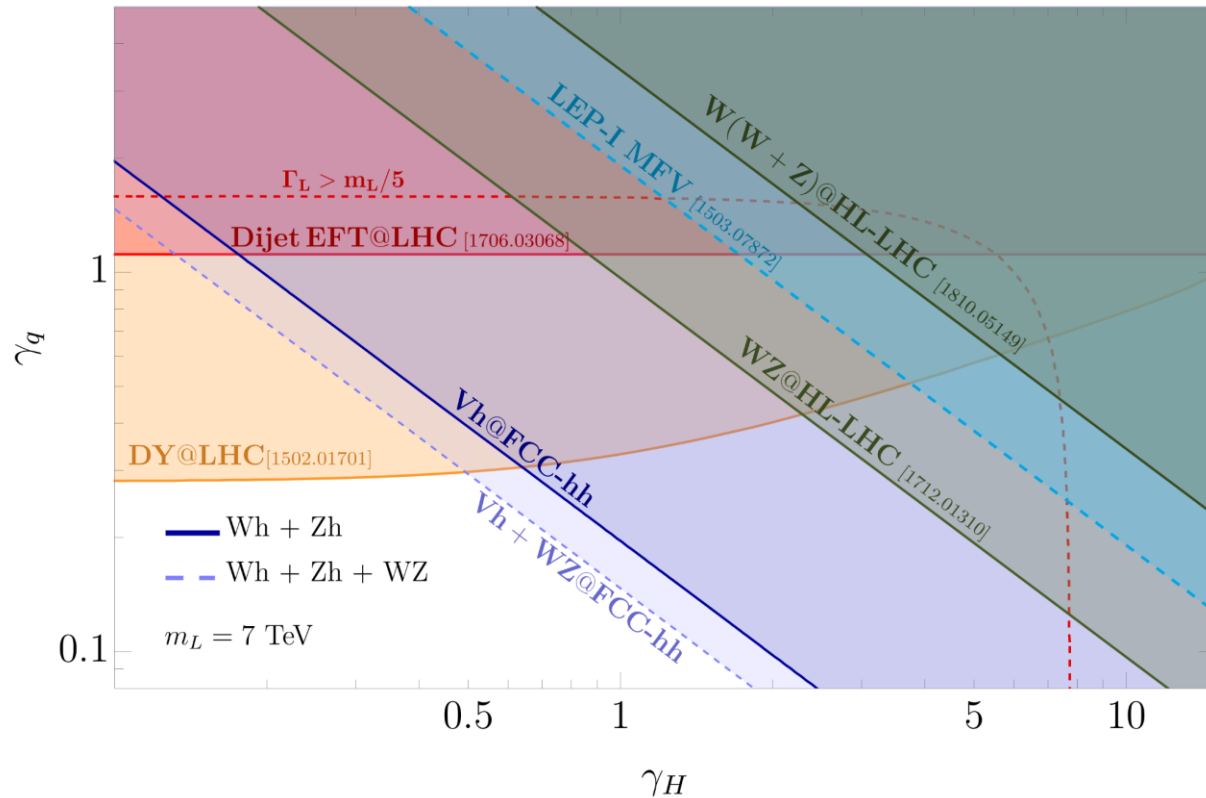
UV models: Spin-1 triplets

$$L_\mu \sim (1, 3)_0$$

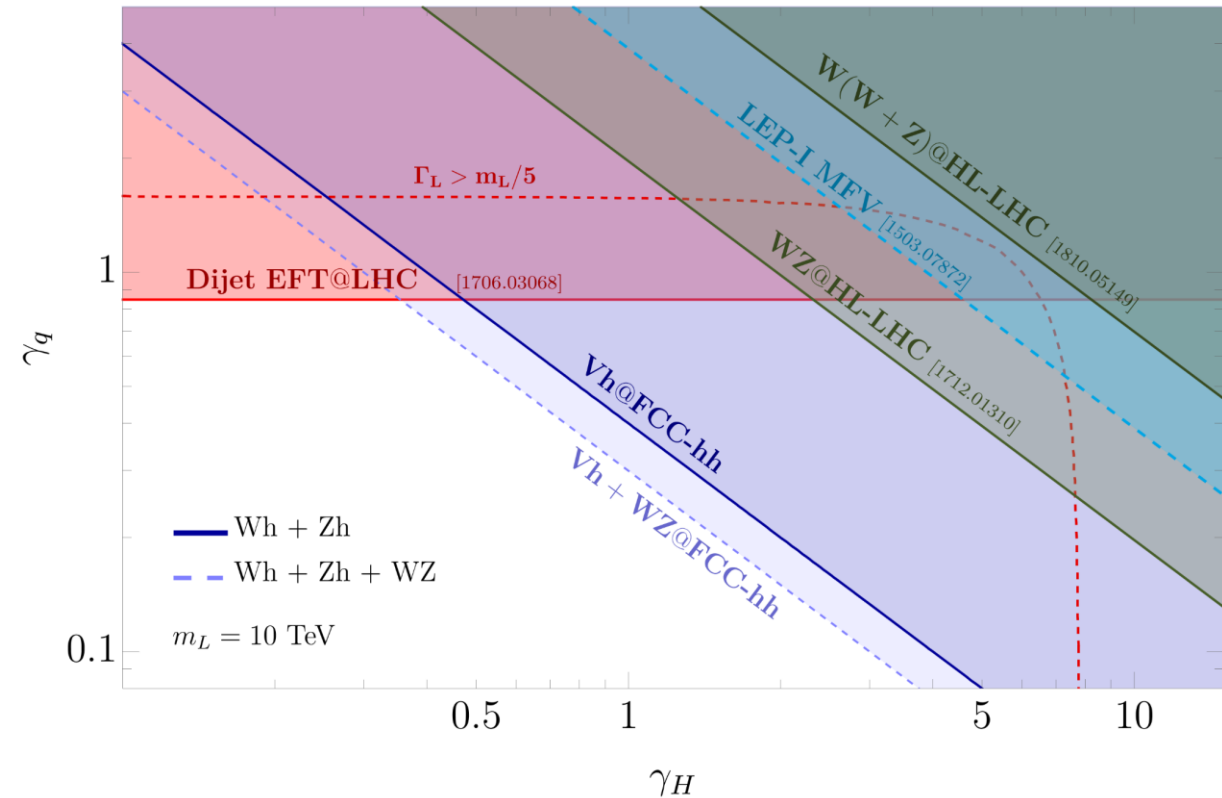
$$\mathcal{L}_{BSM} = \frac{1}{4} F_{L,\mu\nu}^a F_L^{a,\mu\nu} + \frac{m_L^2}{2} L_\mu L^\mu + \gamma_H L_\mu^a \frac{i}{2} H^\dagger \sigma^a \overleftrightarrow{D}^\mu H + \sum_f \gamma_f L_\mu^a \bar{f} \gamma^\mu \sigma^a f$$

$$c_{\varphi q}^{(3)} = -\frac{\gamma_H \gamma_q}{2m_L^2}$$

FCC-hh 100 TeV 30 ab⁻¹ 5% Syst.



FCC-hh 100 TeV 30 ab⁻¹ 5% Syst.

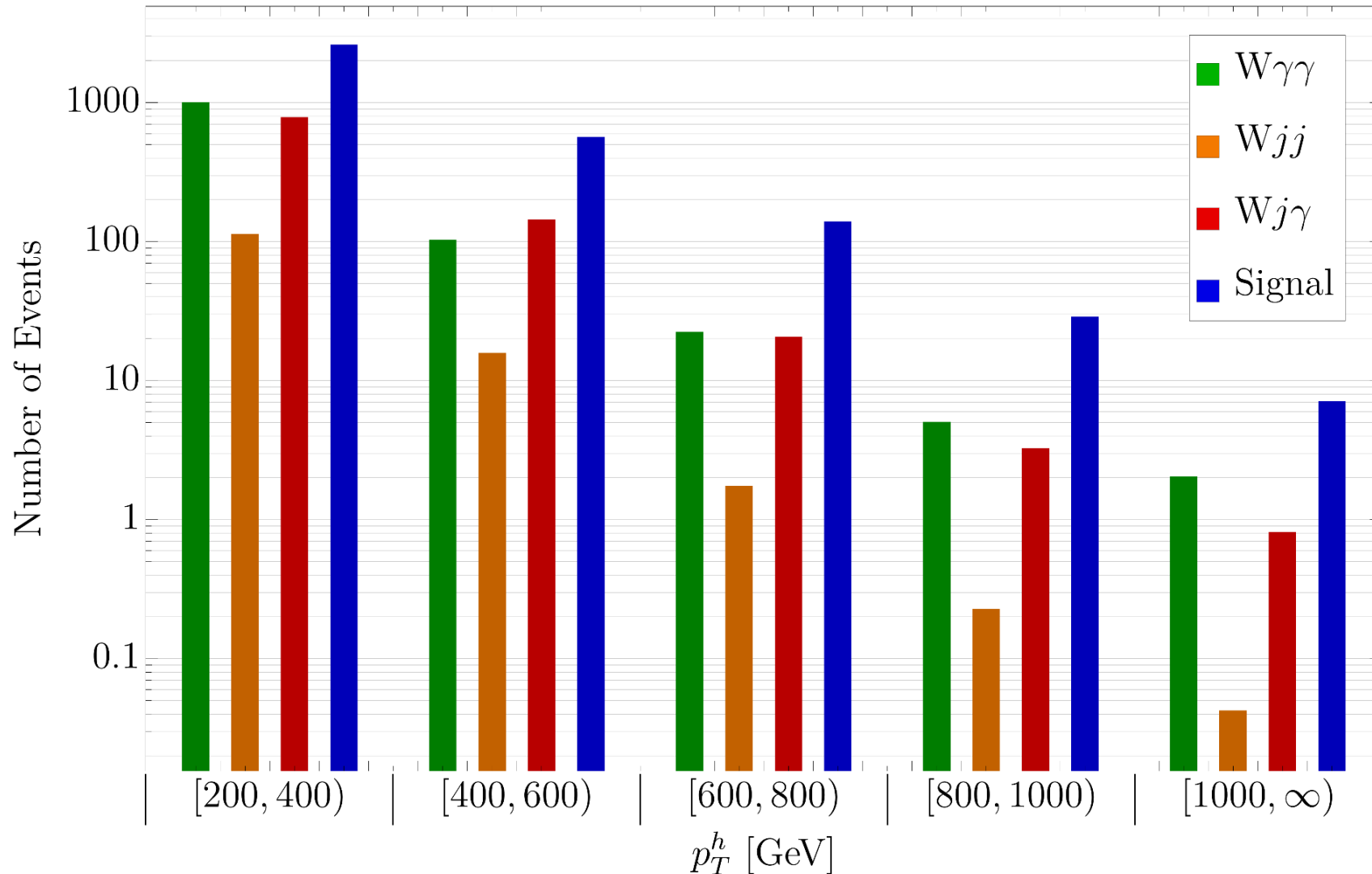


Wh.

How big is the background?

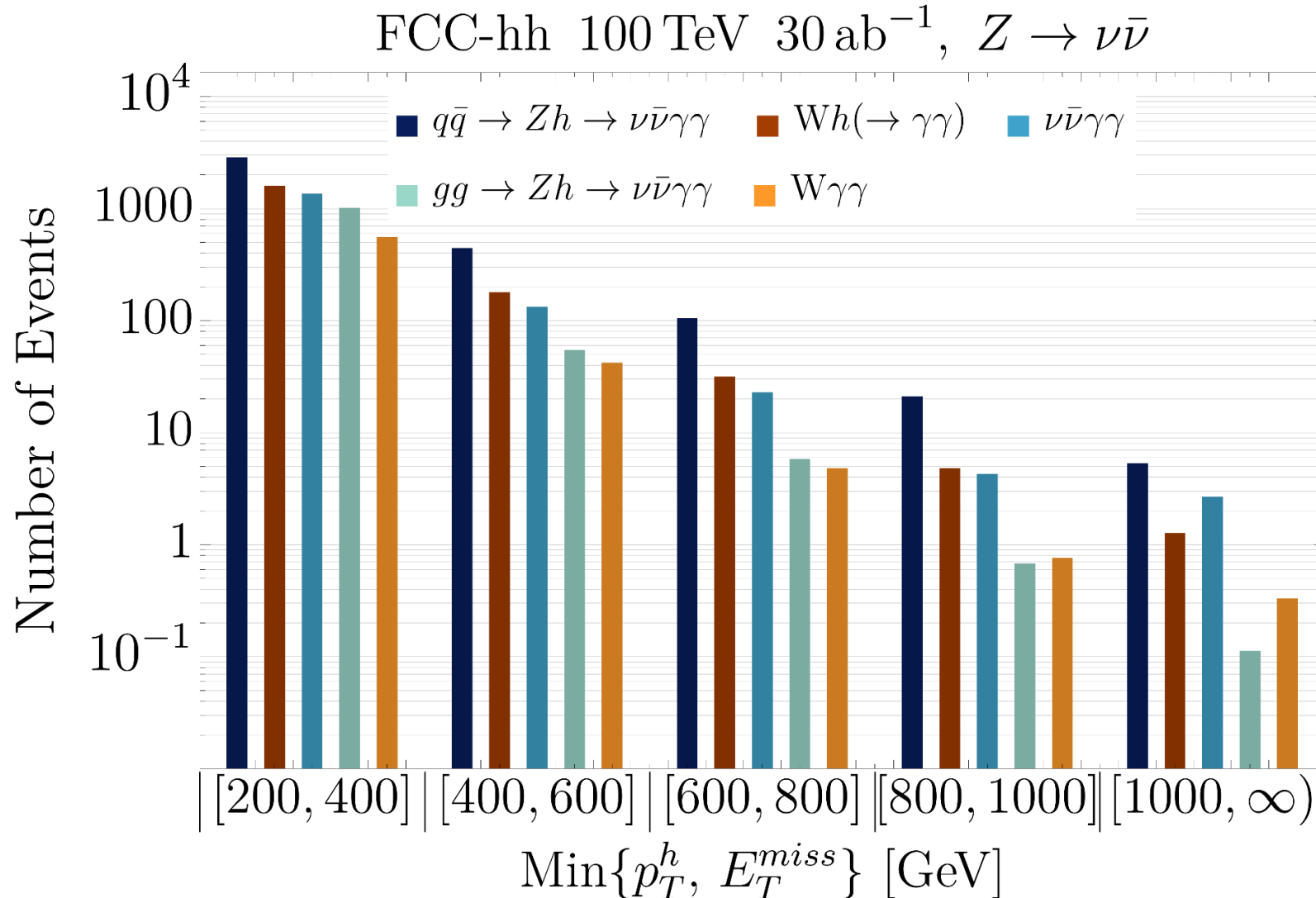
- Events per bin for the relevant processes

FCC-hh 100 TeV 30 ab⁻¹



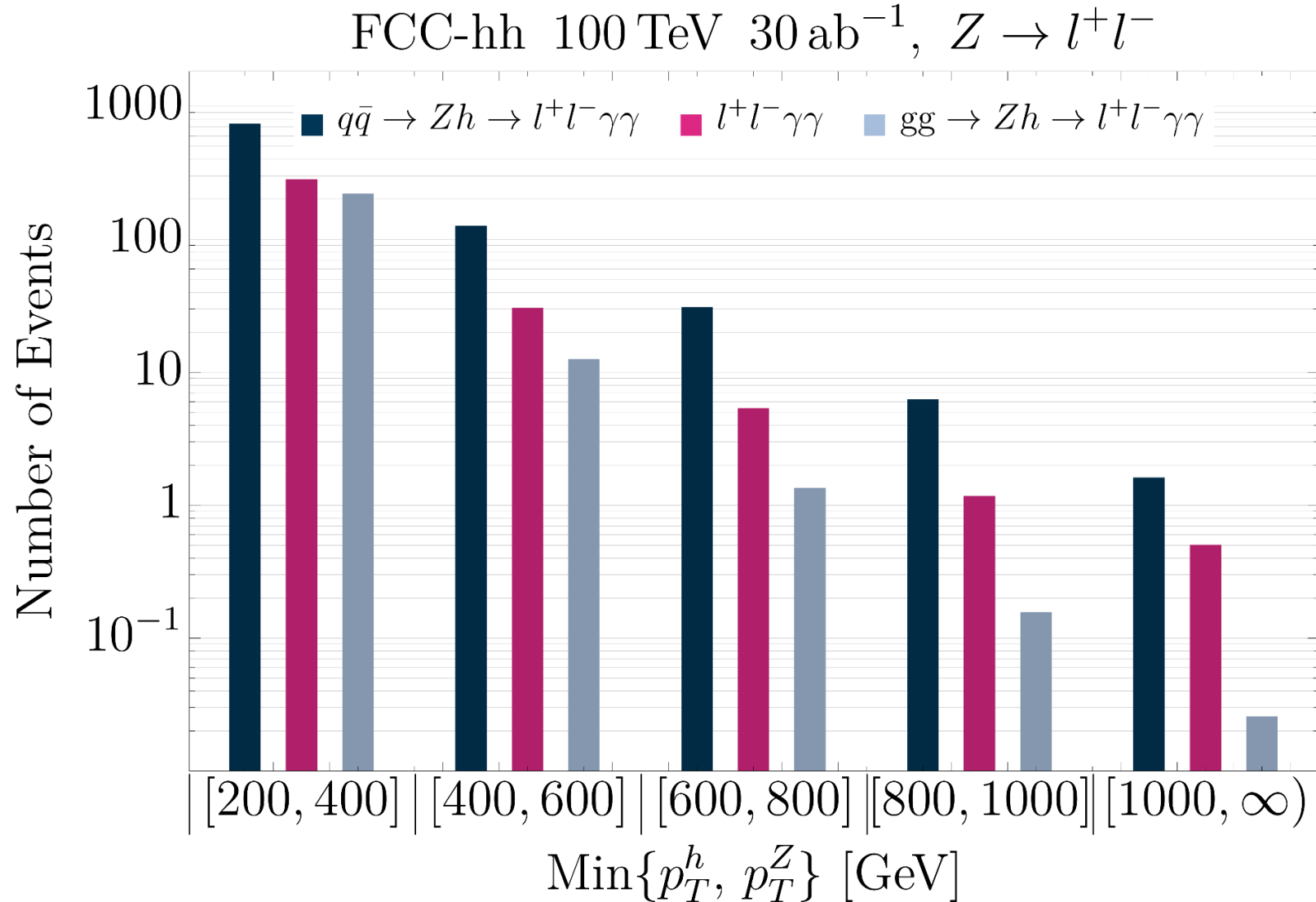
Signal and background

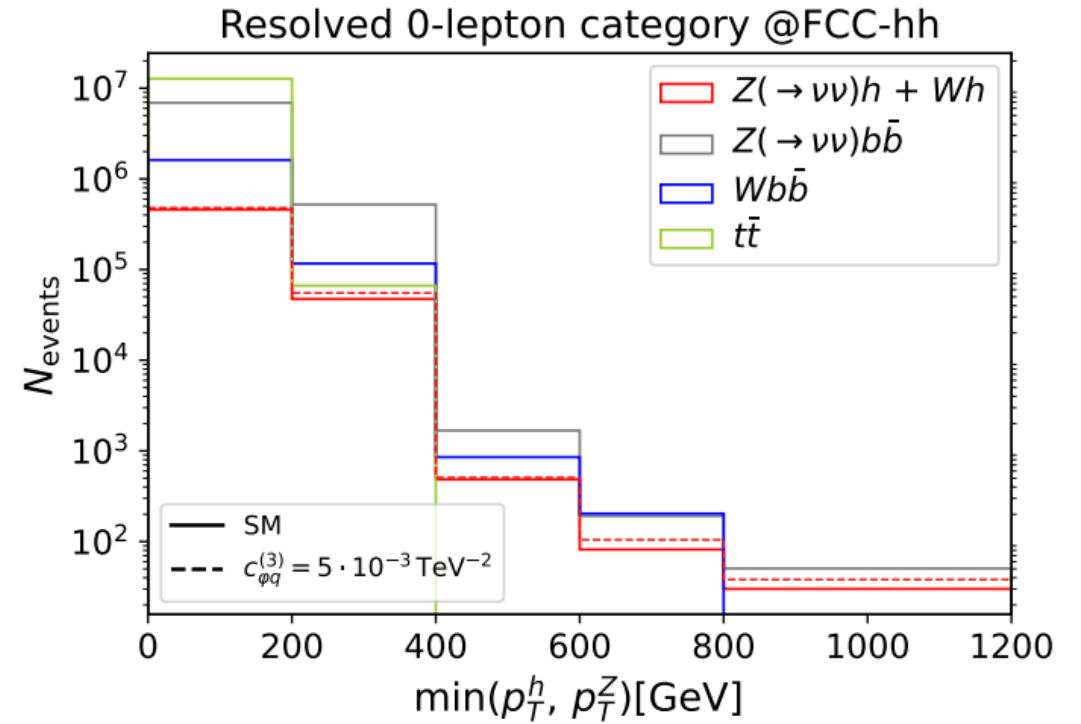
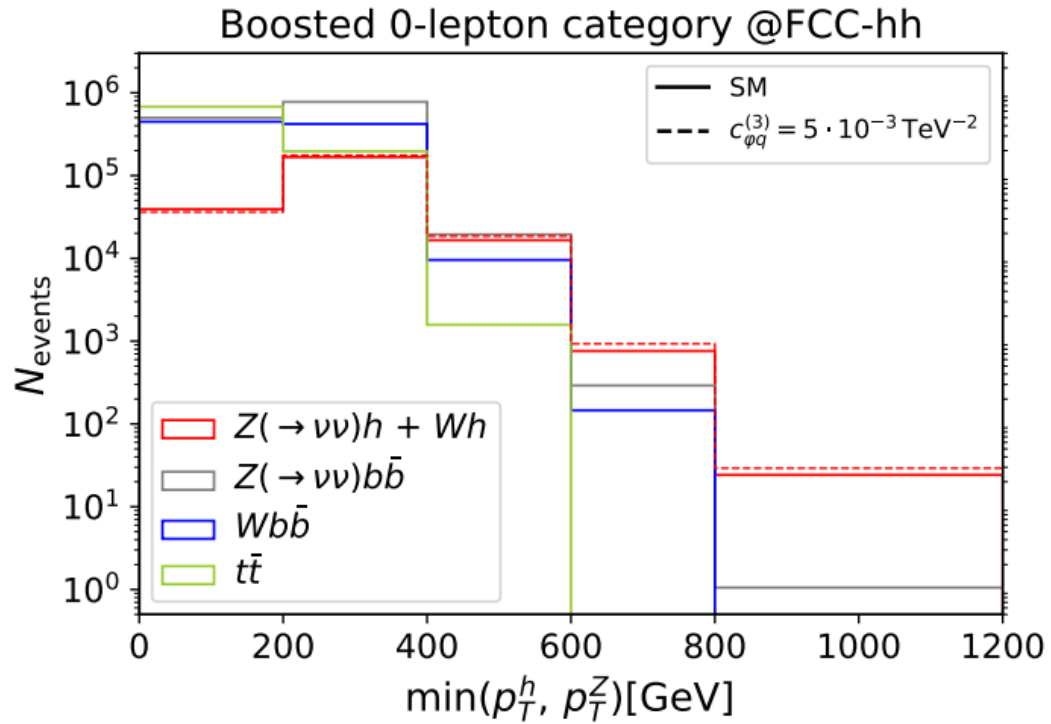
- Wh is part of the signal because it is affected by $\mathcal{O}_{\varphi q}^{(3)}$.

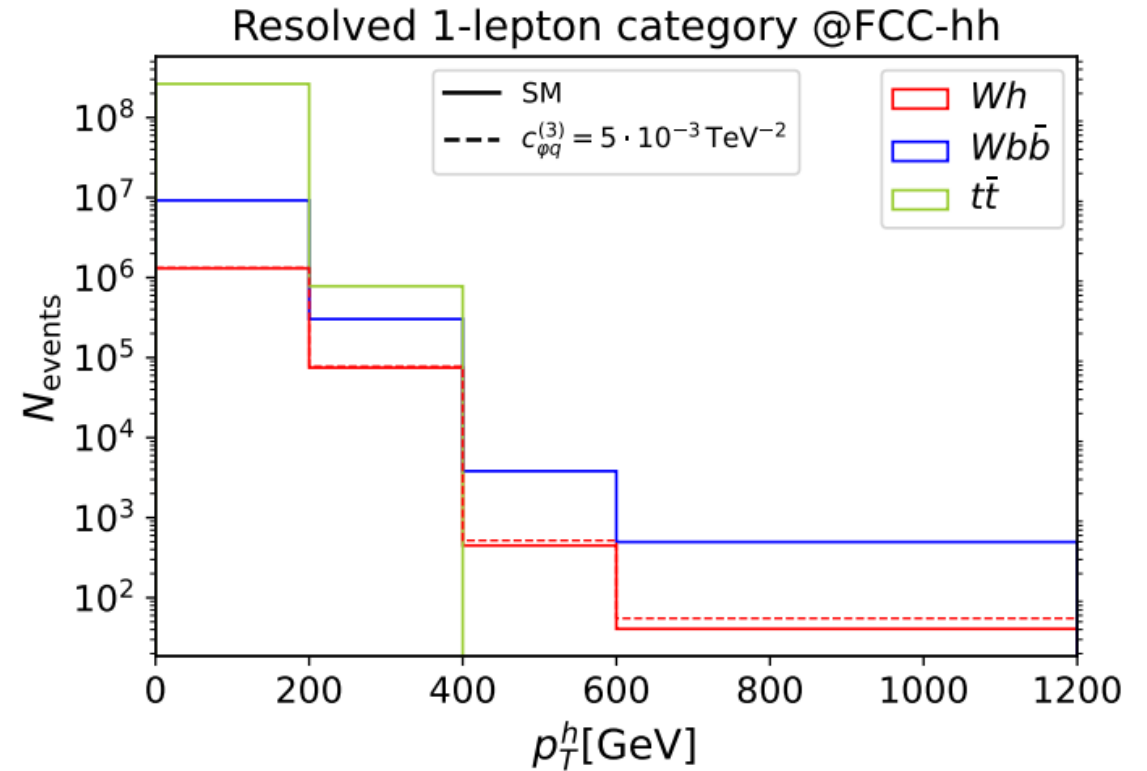
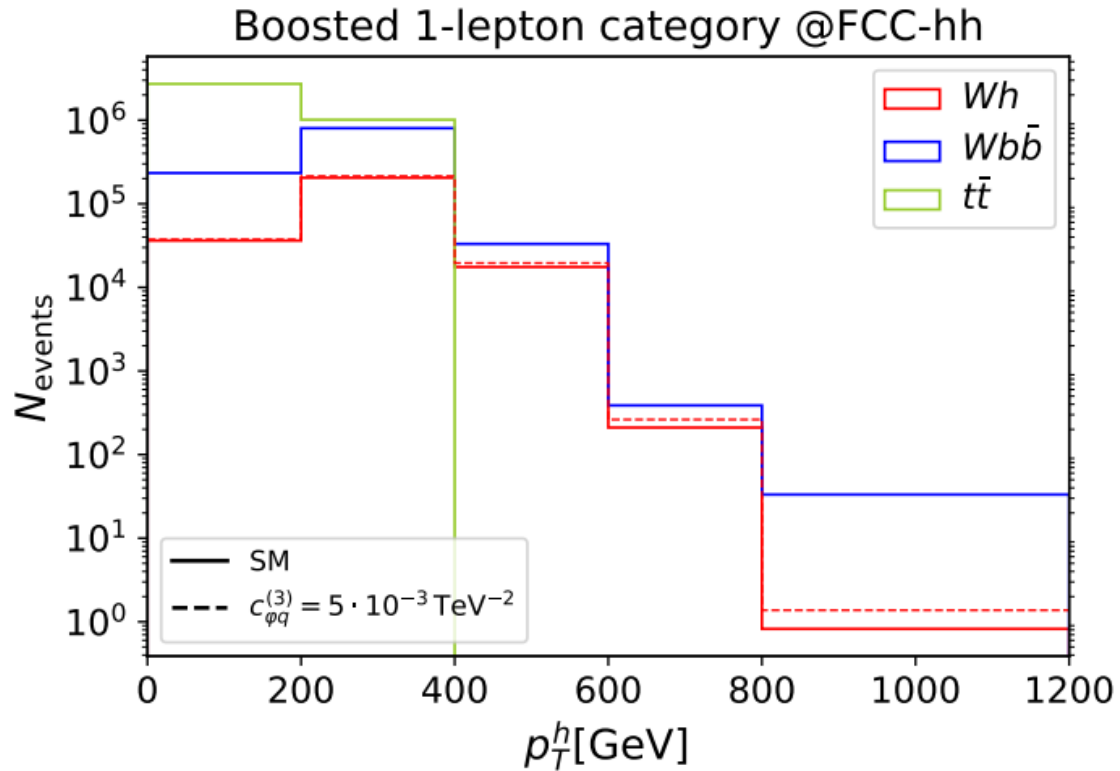


More results

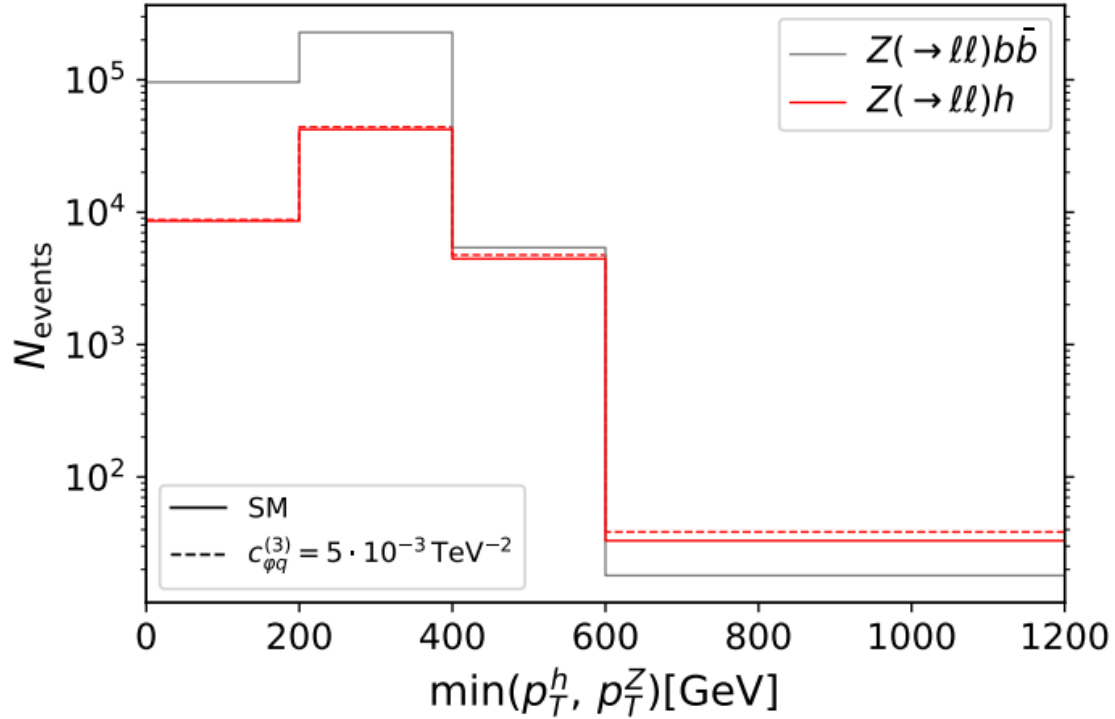
- Events per bin for the relevant processes in the leptonic channel.



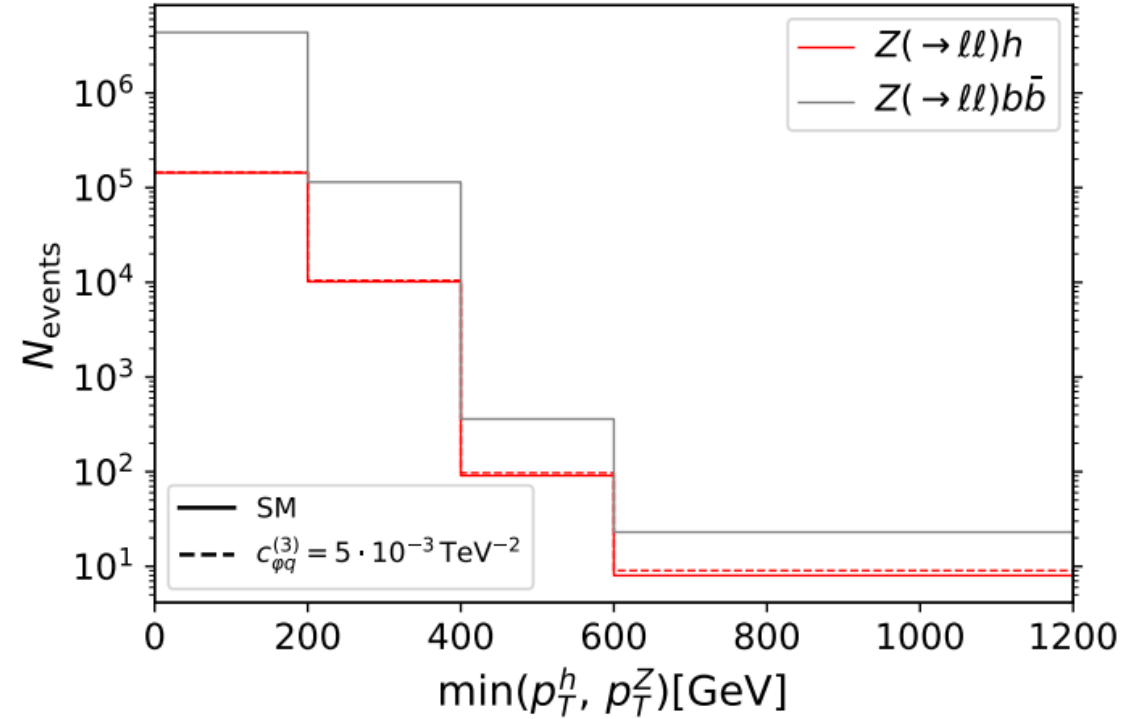




Boosted 2-lepton category @FCC-hh



Resolved 2-lepton category @FCC-hh



Vh

$h \rightarrow b\bar{b}$

Coefficient	Profiled Fit		One-Operator Fit	
$c_{\varphi q}^{(3)}$ [TeV ⁻²]	$[-2.0, 2.1] \times 10^{-3}$	1% syst.	$[-1.1, 1.1] \times 10^{-3}$	1% syst.
	$[-4.9, 3.7] \times 10^{-3}$	5% syst.	$[-2.5, 2.4] \times 10^{-3}$	5% syst.
	$[-7.6, 5.1] \times 10^{-3}$	10% syst.	$[-4.0, 3.6] \times 10^{-3}$	10% syst.
$c_{\varphi q}^{(1)}$ [TeV ⁻²]	$[-10.6, 9.0] \times 10^{-3}$	1% syst.	$[-8.2, 8.1] \times 10^{-3}$	1% syst.
	$[-14.8, 13.6] \times 10^{-3}$	5% syst.	$[-11.3, 11.5] \times 10^{-3}$	5% syst.
	$[-17.2, 16.4] \times 10^{-3}$	10% syst.	$[-13.1, 13.3] \times 10^{-3}$	10% syst.
$c_{\varphi u}$ [TeV ⁻²]	$[-15.9, 9.0] \times 10^{-3}$	1% syst.	$[-6.2, 4.9] \times 10^{-3}$	1% syst.
	$[-27.0, 13.5] \times 10^{-3}$	5% syst.	$[-24.9, 8.2] \times 10^{-3}$	5% syst.
	$[-30.4, 16.4] \times 10^{-3}$	10% syst.	$[-30.2, 10.4] \times 10^{-3}$	10% syst.
$c_{\varphi d}$ [TeV ⁻²]	$[-17.9, 23.6] \times 10^{-3}$	1% syst.	$[-9.8, 23.0] \times 10^{-3}$	1% syst.
	$[-22.0, 26.5] \times 10^{-3}$	5% syst.	$[-14.0, 24.5] \times 10^{-3}$	5% syst.
	$[-25.1, 29.5] \times 10^{-3}$	10% syst.	$[-16.9, 26.4] \times 10^{-3}$	10% syst.

- 95% CL bounds summary

Coefficient	Profiled Fit		One Operator Fit	
$c_{\varphi q}^{(3)}$	$[-5.1, 3.4] \times 10^{-3}$	1% syst.	$[-2.7, 2.5] \times 10^{-3}$	1% syst.
	$[-11.6, 3.8] \times 10^{-3}$	5% syst.	$[-3.3, 2.9] \times 10^{-3}$	5% syst.
	$[-20.6, 4.1] \times 10^{-3}$	10% syst.	$[-4.0, 3.5] \times 10^{-3}$	10% syst.
$c_{\varphi W}$	$[-7.1, 7.9] \times 10^{-2}$	1% syst.	$[-5.3, 4.3] \times 10^{-2}$	1% syst.
	$[-13.0, 17.5] \times 10^{-2}$	5% syst.	$[-12.1, 6.8] \times 10^{-2}$	5% syst.
	$[-20.0, 25.2] \times 10^{-2}$	10% syst.	$[-18.8, 9.0] \times 10^{-2}$	10% syst.
$c_{\varphi \tilde{W}}$	$[-6.4, 6.4] \times 10^{-2}$	1% syst.	$[-6.1, 6.1] \times 10^{-2}$	1% syst.
	$[-9.0, 8.8] \times 10^{-2}$	5% syst.	$[-8.1, 8.1] \times 10^{-2}$	5% syst.
	$[-13.5, 14.2] \times 10^{-2}$	10% syst.	$[-10.1, 10.1] \times 10^{-2}$	10% syst.

- 95% CL bounds summary

Coefficient	Profiled Fit	One Operator Fit
$c_{\varphi q}^{(3)}$	$[-5.2, 3.1] \times 10^{-3}$ 1% syst.	$[-2.1, 2.0] \times 10^{-3}$ 1% syst.
	$[-6.7, 3.3] \times 10^{-3}$ 5% syst.	$[-2.6, 2.4] \times 10^{-3}$ 5% syst.
	$[-8.2, 3.7] \times 10^{-3}$ 10% syst.	$[-3.2, 2.8] \times 10^{-3}$ 10% syst.
$c_{\varphi q}^{(3)}$ (+Wh)	$[-2.5, 2.1] \times 10^{-3}$ 1% syst.	$[-1.6, 1.6] \times 10^{-3}$ 1% syst.
	$[-3.0, 2.4] \times 10^{-3}$ 5% syst.	$[-2.0, 1.9] \times 10^{-3}$ 5% syst.
	$[-3.7, 2.7] \times 10^{-3}$ 10% syst.	$[-2.4, 2.2] \times 10^{-3}$ 10% syst.
$c_{\varphi q}^{(1)}$	$[-1.3, 1.4] \times 10^{-2}$ 1% syst.	$[-1.1, 1.15] \times 10^{-2}$ 1% syst.
	$[-1.5, 1.5] \times 10^{-2}$ 5% syst.	$[-1.1, 1.2] \times 10^{-2}$ 5% syst.
	$[-1.6, 1.5] \times 10^{-2}$ 10% syst.	$[-1.2, 1.2] \times 10^{-2}$ 10% syst.
$c_{\varphi u}$	$[-2.0, 1.6] \times 10^{-2}$ 1% syst.	$[-1.9, 0.89] \times 10^{-2}$ 1% syst.
	$[-2.1, 1.7] \times 10^{-2}$ 5% syst.	$[-2.1, 0.96] \times 10^{-2}$ 5% syst.
	$[-2.2, 1.8] \times 10^{-2}$ 10% syst.	$[-2.2, 1.0] \times 10^{-2}$ 10% syst.
$c_{\varphi d}$	$[-2.1, 2.3] \times 10^{-2}$ 1% syst.	$[-1.4, 2.2] \times 10^{-2}$ 1% syst.
	$[-2.2, 2.4] \times 10^{-2}$ 5% syst.	$[-1.5, 2.2] \times 10^{-2}$ 5% syst.
	$[-2.3, 2.5] \times 10^{-2}$ 10% syst.	$[-1.5, 2.2] \times 10^{-2}$ 10% syst.

- Selection cuts and binning:

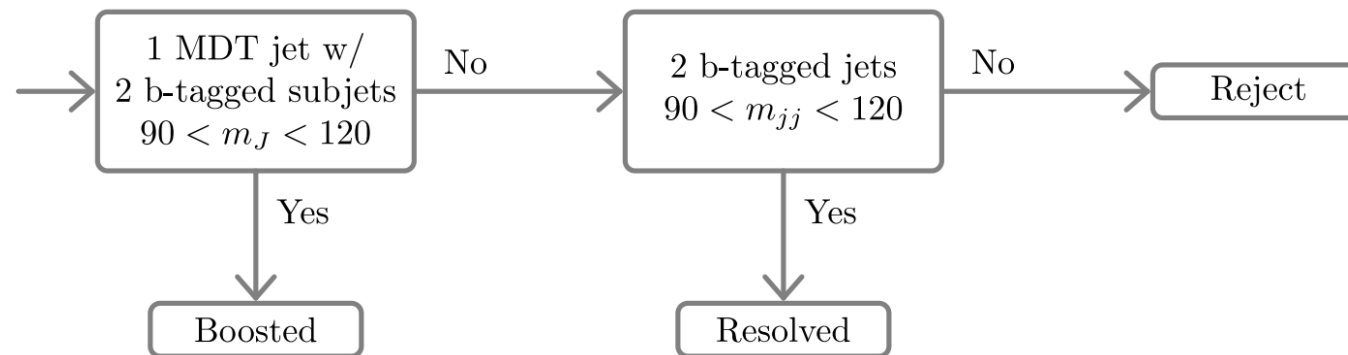
$Z \rightarrow \nu\bar{\nu}$		$Z \rightarrow l^-l^+$	
Bins of $ y^h $	Bins of $\min\{p_T^h, p_T^Z\}$		Bins of $ y^{Zh} $
[0, 2), [2, 6]	[200, 400)		[0, 2), [2, 6]
	[400, 600)		
[0, 1.5), [1.5, 6]	[600, 800)		
[0, 1), [1, 6]	[800, 1000)		
	[1000, ∞)		

	Selection cuts
$p_{T,\min}^l$ [GeV]	30
$p_{T,\min}^\gamma$ [GeV]	50
$m_{\gamma\gamma}$ [GeV]	[120, 130]
m_{l+l^-} [GeV]	[81, 101]
$\Delta R_{\max}^{\gamma\gamma}$	{1.3, 0.9, 0.75, 0.6, 0.6}
$\Delta R_{\max}^{l+l^-}$	{1.2, 0.8, 0.6, 0.5, 0.4}
$p_{T,\max}^{Zh}$ [GeV]	{200, 600, 1100, 1500, 1900}

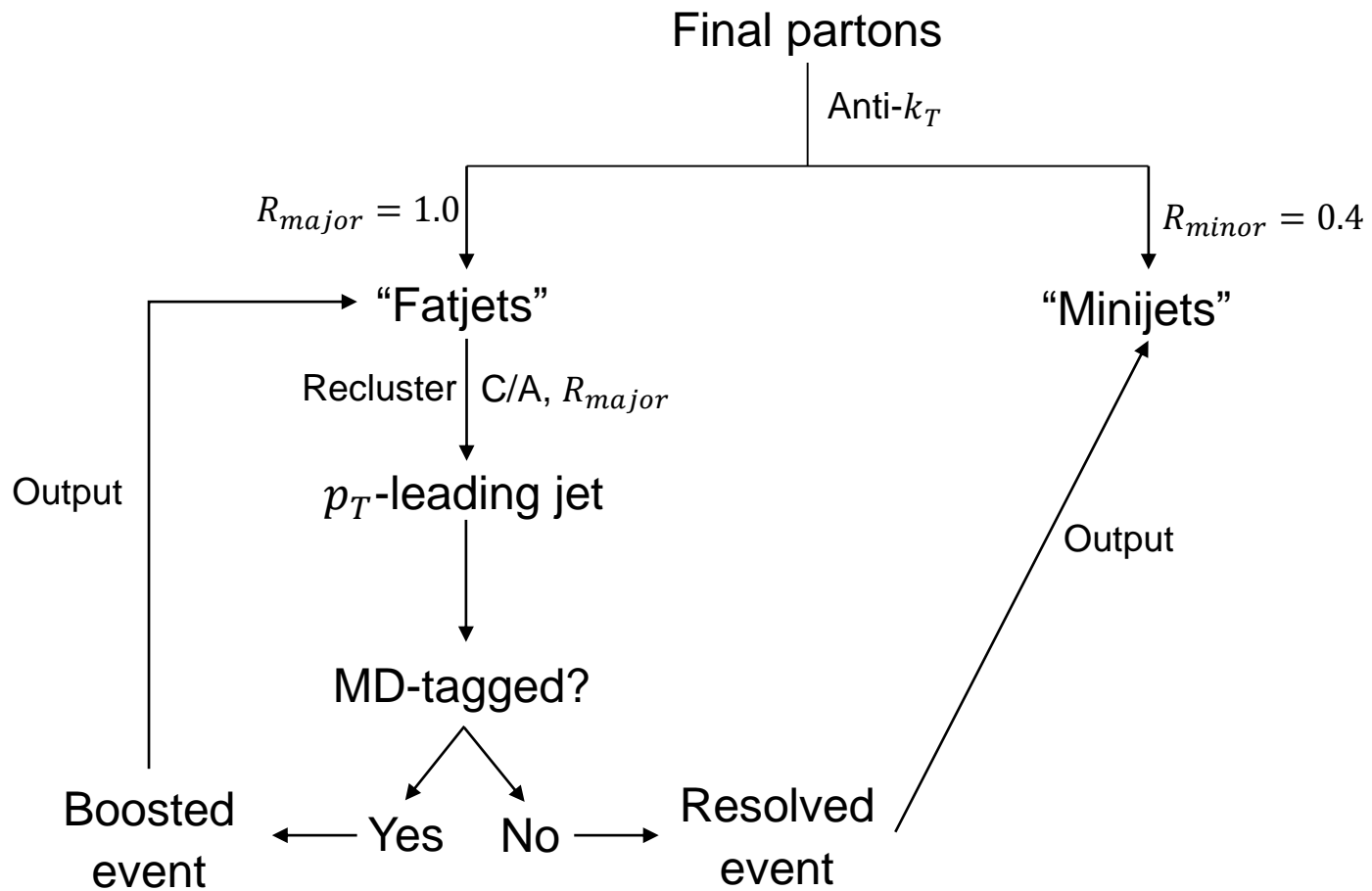
- K-factors for signal in 1+QCD+QED format

p_{Tmin} bin [GeV]	$Zh \rightarrow ll\gamma\gamma$	$Zh \rightarrow \nu\nu\gamma\gamma$	$Wh \rightarrow \nu l\gamma\gamma$
0 – 200	$1 + 0.59 - 0.07 = 1.52$	$1 + 0.26 - 0.06 = 1.20$	$1 + 0.17 - 0.04 = 1.13$
200 – 400	$1 + 0.52 - 0.09 = 1.43$	$1 + 0.31 - 0.09 = 1.22$	$1 + 0.28 - 0.09 = 1.19$
400 – 600	$1 + 0.64 - 0.14 = 1.50$	$1 + 0.37 - 0.14 = 1.23$	$1 + 0.28 - 0.17 = 1.11$
600 – 800	$1 + 0.69 - 0.18 = 1.51$	$1 + 0.40 - 0.18 = 1.22$	$1 + 0.35 - 0.24 = 1.11$
800 – 1000	$1 + 0.70 - 0.24 = 1.46$	$1 + 0.40 - 0.24 = 1.16$	$1 + 0.39 - 0.32 = 1.07$
1000 – ∞	$1 + 0.69 - 0.32 = 1.37$	$1 + 0.40 - 0.32 = 1.08$	$1 + 0.36 - 0.40 = 0.96$

Tagging algorithm



Tagging algorithm



(b-)Tagging algorithm

$\exists (b, c, j)$ final parton within $\Delta R \leq R_{minor}$ of Minijet \longrightarrow b -tag for Minijet with prob. $eff_{(b,c,j)}^{LHC/FCC}$

For Boosted events

Enough for Resolved events

+1 b -tag for MDT jet per b -tagged Minijet within $\Delta R \leq 0.2$

$$eff_b^{LHC} = \begin{cases} 0 & \text{if } p_T \leq 20 \text{ GeV or } |\eta| > 2.5 \\ 0.8 \tanh(0.003 p_T) \frac{30}{1+0.086 p_T} & \text{else} \end{cases}$$

$$eff_c^{LHC} = \begin{cases} 0 & \text{if } p_T \leq 20 \text{ GeV or } |\eta| > 2.5 \\ 0.2 \tanh(0.02 p_T) \frac{1}{1+0.0034 p_T} & \text{else} \end{cases}$$

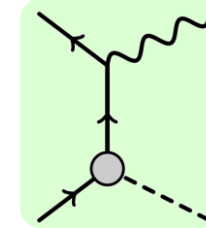
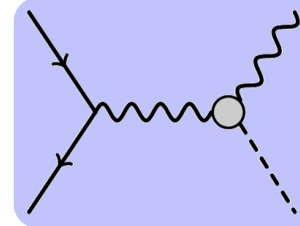
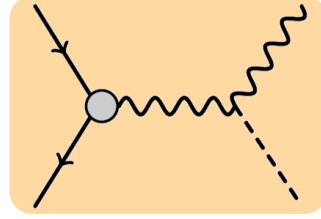
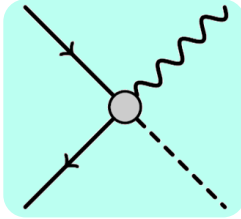
$$eff_j^{LHC} = \begin{cases} 0 & \text{if } p_T \leq 20 \text{ GeV or } |\eta| > 2.5 \\ 0.002 \tanh(7.3 \cdot 10^{-6} \cdot p_T) & \text{else} \end{cases}$$

$$eff_b^{FCC} = \begin{cases} 0 & \text{if } p_T \leq 20 \text{ GeV or } |\eta| > 4.5 \\ 0.85 & \text{else} \end{cases}$$

$$eff_c^{FCC} = \begin{cases} 0 & \text{if } p_T \leq 20 \text{ GeV or } |\eta| > 4.5 \\ 0.05 & \text{else} \end{cases}$$

$$eff_j^{FCC} = \begin{cases} 0 & \text{if } p_T \leq 20 \text{ GeV or } |\eta| > 4.5 \\ 0.01 & \text{else} \end{cases}$$

Dimension-6 operators in Vh



$$\mathcal{O}_{\varphi D} = (H^\dagger D^\mu H)^* (H^\dagger D_\mu H)$$

$$\mathcal{O}_{\varphi W} = H^\dagger H W^{a,\mu\nu} W_{\mu\nu}^a$$

$$\mathcal{O}_{\varphi \tilde{W}} = H^\dagger H W^{a,\mu\nu} \tilde{W}_{\mu\nu}^a$$

$$\mathcal{O}_{\varphi B} = H^\dagger H B^{\mu\nu} B_{\mu\nu}$$

$$\mathcal{O}_{\varphi \tilde{B}} = H^\dagger H B^{\mu\nu} \tilde{B}_{\mu\nu}$$

$$\mathcal{O}_{\varphi WB} = H^\dagger \sigma^a H B^{\mu\nu} W_{\mu\nu}^a$$

$$\mathcal{O}_{\varphi \tilde{W}B} = H^\dagger \sigma^a H B^{\mu\nu} \tilde{W}_{\mu\nu}^a$$

$$\mathcal{O}_{uW} = (\bar{q}_L \sigma^{\mu\nu} u_R) \tau^I \tilde{H} W_{\mu\nu}^I$$

$$\mathcal{O}_{dW} = (\bar{q}_L \sigma^{\mu\nu} d_R) \tau^I H W_{\mu\nu}^I$$

$$\mathcal{O}_{uB} = (\bar{q}_L \sigma^{\mu\nu} u_R) \tilde{H} B_{\mu\nu}$$

$$\mathcal{O}_{dB} = (\bar{q}_L \sigma^{\mu\nu} d_R) H B_{\mu\nu}$$

$$\mathcal{O}_{\varphi ud} = (\bar{u}_R \gamma^\mu d_R) \left(i H^\dagger \overleftrightarrow{D}_\mu H \right)$$

$$\mathcal{O}_{\varphi q}^{(3)} = (\bar{Q}_L \sigma^a \gamma^\mu Q_L) \left(i H^\dagger \sigma^a \overleftrightarrow{D}_\mu H \right)$$

$$\mathcal{O}_{\varphi q}^{(1)} = (\bar{Q}_L \gamma^\mu Q_L) \left(i H^\dagger \overleftrightarrow{D}_\mu H \right)$$

$$\mathcal{O}_{\varphi u} = (\bar{u}_R \gamma^\mu u_R) \left(i H^\dagger \overleftrightarrow{D}_\mu H \right)$$

$$\mathcal{O}_{\varphi d} = (\bar{d}_R \gamma^\mu d_R) \left(i H^\dagger \overleftrightarrow{D}_\mu H \right)$$

$$\mathcal{O}_{u\varphi} = H^\dagger H (\bar{q}_L \tilde{H} u_R)$$

$$\mathcal{O}_{d\varphi} = H^\dagger H (\bar{q}_L H d_R)$$

—— MFV suppressed
 —— Sub-leading energy growth
 —— No interference with SM for massless quarks